






## Article

# Advanced Path Planning for UAV Swarms in Smart City Disaster Scenarios Using Hybrid Metaheuristic Algorithms

Mohammed Sani Adam <sup>1,2</sup>, Nor Fadzilah Abdullah <sup>1,2</sup>, Asma Abu-Samah <sup>1,2</sup>, Oluwatosin Ahmed Amodu <sup>3</sup>  
and Rosdiadee Nordin <sup>4,\*</sup>

<sup>1</sup> Department of Electrical, Electronic and Systems Engineering, Faculty of Engineering and Built Environment, Universiti Kebangsaan Malaysia, Bangi 43600, Malaysia; p106820@siswa.ukm.edu.my (M.S.A.); fadzilah.abdullah@ukm.edu.my (N.F.A.); asma@ukm.edu.my (A.A.-S.)

<sup>2</sup> Wireless Research@UKM, Department of Electrical, Electronic and Systems Engineering, Faculty of Engineering and Built Environment, Universiti Kebangsaan Malaysia, Bangi 43600, Malaysia

<sup>3</sup> Department of Communication Technology and Network, Universiti Putra Malaysia (UPM), Serdang 43400, Malaysia; oluwatosinahmed@upm.edu.my

<sup>4</sup> School of Engineering and Technology, Sunway University, 5, Jalan Universiti, Bandar Sunway 47500, Malaysia

\* Correspondence: rosdiadeen@sunway.edu.my

**Abstract:** In disaster-stricken areas, rapid restoration of communication infrastructure is critical to ensuring effective emergency response and recovery. Swarm UAVs, operating as mobile aerial base stations (MABS), offer a transformative solution for bridging connectivity gaps in environments where the traditional infrastructure has been compromised. This paper presents a novel hybrid path planning approach combining affinity propagation clustering (APC) with genetic algorithms (GA), aimed at maximizing coverage, and ensuring quality of service (QoS) compliance across diverse environmental conditions. Comprehensive simulations conducted in suburban, urban, dense urban, and high-rise urban environments demonstrated the efficacy of the APC-GA approach. The proposed method achieved up to 100% coverage in suburban settings with only eight unmanned aerial vehicle (UAV) swarms, and maintained superior performance in dense and high-rise urban environments, achieving 97% and 93% coverage, respectively, with 10 UAV swarms. The QoS compliance reached 98%, outperforming benchmarks such as GA (94%), PSO (90%), and ACO (88%). The solution exhibited significant stability, maintaining consistently high performance, highlighting its robustness under dynamic disaster scenarios. Mobility model analysis further underscores the adaptability of the proposed approach. The reference point group mobility (RPGM) model consistently achieved higher coverage rates (95%) than the random waypoint model (RWPM) (90%), thereby demonstrating the importance of group-based mobility patterns in enhancing UAV deployment efficiency. The findings reveal that the APC-GA adaptive clustering and path planning mechanisms effectively navigate propagation challenges, interference, and non-line-of-sight (NLOS) conditions, ensuring reliable connectivity in the most demanding environments. This research establishes the APC-GA hybrid as a scalable and QoS-compliant solution for UAV deployment in disaster response scenarios. By dynamically adapting to environmental complexities and user mobility patterns, it advances state-of-the-art emergency communication systems, offering a robust framework for real-world applications in disaster resilience and recovery.

**Keywords:** UAV swarms; path optimization; disaster response; hybrid algorithms; Affinity Propagation Clustering; Genetic Algorithm



Academic Editor: Diego González-Aguilera

Received: 12 December 2024

Revised: 13 January 2025

Accepted: 13 January 2025

Published: 16 January 2025

**Citation:** Adam, M.S.; Abdullah, N.F.; Abu-Samah, A.; Amodu, O.A.; Nordin, R. Advanced Path Planning for UAV Swarms in Smart City Disaster Scenarios Using Hybrid Metaheuristic Algorithms. *Drones* **2025**, *9*, 64. <https://doi.org/10.3390/drones9010064>

**Copyright:** © 2025 by the authors. Licensee MDPI, Basel, Switzerland.

This article is an open access article distributed under the terms and conditions of the Creative Commons Attribution (CC BY) license (<https://creativecommons.org/licenses/by/4.0/>).

## 1. Introduction

Using unmanned aerial vehicles (UAV) swarms as mobile aerial base stations (MABSs) has become a transformative solution for providing emergency communications in disaster scenarios. Unlike conventional ground-based systems, UAVs offer unparalleled flexibility and adaptability, particularly when terrestrial infrastructure is damaged or unavailable. UAV swarms can deliver enhanced coverage and reliable connectivity by utilizing line-of-sight (LOS) communication and dynamic aerial positioning [1]. Historical examples, such as the deployment of cell-on-wings (COW) drones during Hurricane Maria in Puerto Rico, highlight the critical role of UAVs in restoring cellular services and supporting disaster recovery operations. These systems ensure real-time data transmission and reduce dependency on costly and vulnerable terrestrial networks. However, optimizing the deployment and path planning of UAV swarms to maintain efficient and uninterrupted coverage remains a significant challenge [2].

Achieving reliable broadband connectivity is essential for emergency management and public safety in disaster response networks (DRNs). Infrastructure disruptions often lead to network congestion, particularly in areas where displaced populations are concentrated in protected zones. Traditional base stations are either rendered inoperative or overwhelmed by increased traffic. UAV swarms can mitigate these issues by dynamically adapting their positions to extend coverage across the affected regions. Although existing approaches demonstrate the potential benefits of MABS deployment (see Section 2), more robust and efficient algorithms are needed to address the unique challenges posed by dynamic user mobility, varying population densities, and energy constraints in such environments.

### 1.1. Problem Identification and Novelty

This study addresses the problem of optimizing UAV swarm paths for disaster response scenarios where existing infrastructure is partially or fully compromised. The goal is to ensure comprehensive communication coverage and adapting to dynamic user mobility. In disaster-affected regions, UAV swarms must balance factors such as QoS requirements, user demand variability, and geographical constraints. For example, low-altitude UAVs may be suitable for serving sparsely populated areas, whereas high-density regions with greater communication demands require coordinated and energy-efficient swarm operations.

Existing optimization techniques, such as genetic algorithms (GA) and particle swarm optimization (PSO), have been explored for path planning. However, these methods often fail to account for the critical real-time user dynamics in disaster scenarios. To overcome these limitations, this paper introduces a novel affinity propagation clustering (APC)-GA hybrid algorithm, which combines dynamic clustering with UAV-specific adaptations of genetic operations. The proposed approach ensures real-time path optimization, effectively addressing the following key challenges:

- **Seamless user allocation:** In disaster zones, users frequently move between service areas, creating challenges for maintaining uninterrupted connectivity. Optimized UAV paths are required to dynamically adapt to user transitions.
- **Coverage maximization:** Traditional UAV routing strategies often focus on cluster centroids, potentially neglecting users located in peripheral areas. This study emphasizes a routing approach that ensures complete coverage while maintaining energy efficiency.

### 1.2. Novel Contributions and Approach

The research presented in this paper builds upon existing work by introducing a comprehensive framework for UAV swarm path optimization. Key contributions include the following (Figure 1):

- Contribution 1: A QoS-aware fitness function for UAV swarm optimization: A multi-metric fitness function is proposed, integrating path length, and signal-to-interference-plus-noise ratio (SINR-based) QoS compliance. This ensures that UAVs maintain efficient and interference-free communication while minimizing resource consumption.
- Contribution 2: An APC-GA hybrid framework for UAV path planning: The paper introduces a novel hybrid algorithm that utilizes APC for dynamic user grouping and customized mutation operators for UAV-specific optimization. These enhancements improve adaptability and efficiency in complex environments.
- Contribution 3: Real-time mobility integration: The proposed framework incorporates user mobility into the clustering and optimization process, enabling UAV swarms to dynamically adjust their paths and maintain consistent coverage as user distributions change.

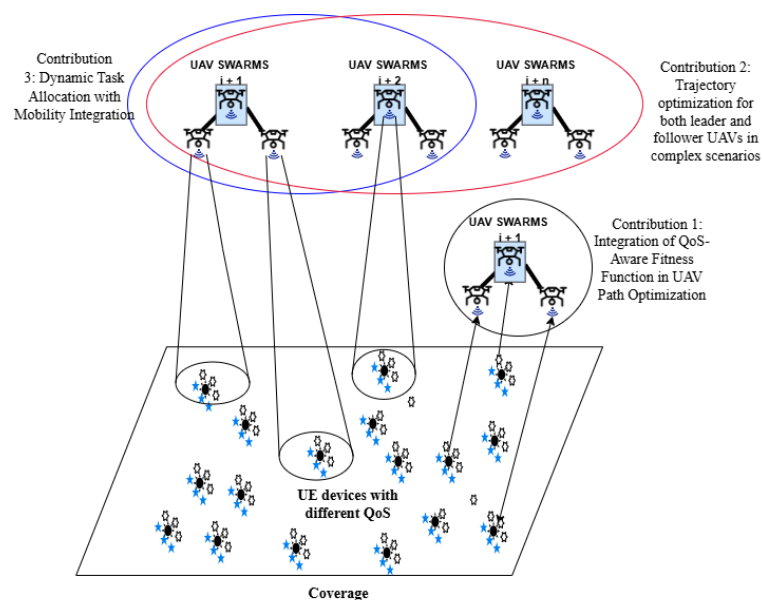


**Figure 1.** Key Contributions of the Study.

### 1.3. Organization of This Paper

The remainder of this paper is structured as follows. Section 2 provides an overview of UAV swarm applications in disaster response, emphasizing the challenges in dynamic path planning. Section 3 describes the environment modeling, path loss modeling, problem definition, and parameter settings. Section 4 details the APC-GA hybrid algorithm, including the fitness function, clustering methodology, and genetic operations. Section 5 presents a comparative evaluation of the proposed approach with the existing methods in urban and suburban disaster scenarios. Finally, Section 6 discusses the findings and potential future directions.

## 2. Related Works

Research on UAV swarm optimization in disaster scenarios can be broadly categorized into two primary areas based on their alignment with the challenges addressed in this study. The first category encompasses optimization techniques focused on deploying and coordinating UAVs to enhance communication coverage. This includes methods such as

PSO, ant colony optimization (ACO), and GA, which aim to optimize UAV positioning and trajectories to maximize connectivity and minimize interference. The second category includes clustering methods and mobility-aware algorithms that emphasize dynamic resource allocation and adaptive trajectory planning. Techniques such as APC and predictive mobility models are particularly noteworthy because they enable UAV swarms to respond proactively to changing user distributions and environmental conditions. These two domains collectively address the critical challenges of scalability, real-time adaptability, and energy efficiency in UAV-assisted disaster response.

### 2.1. UAV Swarm Optimization Techniques

The field of UAV swarm optimization has seen remarkable progress in recent years [3–12], tackling the challenges of disaster management, remote sensing, and dynamic wireless communication using innovative approaches. Researchers have introduced strategies that balance technical precision with practical impacts in high-stake scenarios by focusing on scalability, energy efficiency, and real-time adaptability [3]. In [4], the authors used PSO swarm intelligence algorithms that which have proven highly effective in disaster response [4]. For instance, a distributed PSO-based exploration algorithm allows UAVs to navigate disaster-hit areas autonomously and efficiently discover victim clusters. This method stands out for its ability to balance energy consumption across UAVs while outperforming traditional trajectory-planning techniques in terms of flexibility and adaptability, which is a crucial advantage in unpredictable environments.

Another breakthrough came with the use of the artificial bee colony (ABC) algorithm by authors in [6,7] to deploy UAV base stations in disaster-stricken zones. This approach optimizes UAV positioning to enhance network coverage and throughput while minimizing deployment costs. In comparative studies, the ABC algorithm outperformed traditional techniques such as GA and hybrid PSO-based methods, making it a top choice for large-scale disaster networks where user connectivity and energy efficiency are vital. Exciting advancements have emerged in deep reinforcement learning (DRL). The authors in [8], proposed a wildfire reconnaissance system utilized a DRL framework integrated with double deep Q-Networks (DDQN) to adjust UAV trajectories dynamically. By responding to real-time risk maps, this approach significantly improves the speed and precision of coverage in high-risk areas, showcasing the potential of DRL to redefine UAV swarm operations in complex disaster scenarios [8,9].

Energy-efficient clustering techniques have played a pivotal role in this regard. The authors in [10] have proposed a swarm intelligence-based localization and clustering (SILC) algorithm, developed for emergency communication, optimized cluster head selection and multi-hop connectivity. This approach effectively reduces routing overhead while extending network lifetime, making it highly relevant for dynamic, resource-constrained environments. Researchers have explored frameworks combining integer linear programming (ILP) with heuristic optimization for large-scale operations in [11]. The proposed approach addresses UAV deployment in remote sensing tasks by optimizing UAVs' number, location, and trajectories of UAVs to balance operational costs and maximize user connectivity [11]. The framework excelled in disaster zones with challenging topographies, such as floods and landslides, proving its versatility in diverse scenarios.

Path planning for complex environments has also seen innovations with the introduction of an improved multi-objective swarm intelligence algorithm (IMSIA). Designed for 3D navigation proposed by authors in [5], this method simultaneously tackled flight-path length and terrain threats, thereby ensuring safer UAV operations in rugged disaster zones [5]. Compared to traditional algorithms such as A\* and Dijkstra [13], IMSIA achieved superior efficiency and reliability, particularly in environments with high navigation com-

plexity. Finally, the authors in [12] proposed the use of hybrid models, which are also becoming increasingly prominent. For instance, combining adaptive genetic algorithms (AGA) and ABC for mission assignment and path planning yielded significant improvements [12]. By balancing energy consumption and maximizing mission success rates, this approach demonstrated its effectiveness in disaster response scenarios involving diverse UAV tasks, such as delivery, surveillance, and communication relays [12].

Despite these advancements, several challenges remain. Integrating real-time constraints such as predictive mobility, communication delays, and environmental variability remains an ongoing area of research. Future work could explore hybrid models that blend swarm intelligence and model-based optimization to address these gaps. Such efforts would help balance scalability, latency, and energy efficiency, ensuring that UAV swarms continue to serve as critical tools for disaster resilience and emergency response.

## 2.2. Clustering Methods in UAV Applications

Clustering techniques are fundamental for effectively managing UAV swarms, particularly in disaster response scenarios with a high demand for efficient communication and resource allocation. These methods help group UAVs or users in a manner that optimizes connectivity, reduces communication overhead, and conserves energy, thereby making them critical for ensuring the scalability and adaptability of UAV networks [14–17].

Density-based approaches for dynamic scenarios—dynamic environments, such as disaster-stricken areas, demand clustering techniques that adapt to rapidly changing conditions. The authors in [14] proposed a swarm-intelligence-driven clustering algorithm based on PSO to optimize cluster formation in UAV-assisted networks. The algorithm prioritized energy efficiency by selecting cluster heads (CHs) that minimized communication costs and balanced the workload among UAVs. This reduces delays and extends the network's operational life, thereby addressing a common challenge in such applications [14]. Traditional k-means and its evolution, a widely used clustering method, has often been the starting point for UAV clustering research due to its simplicity and computational efficiency. However, traditional k-means clustering struggles with dynamically varying cluster sizes and mobility patterns. A trajectory-aware version of k-means was developed by authors in [17] to address this by aligning cluster formation with UAV flight paths. By dynamically reconfiguring clusters in response to disaster conditions, this method reduces communication blackouts and improves coverage reliability, demonstrating its potential in high-density scenarios [17].

Three-dimensional clustering for complex environments: In disaster scenarios characterized by uneven terrain or urban landscapes, clustering techniques must operate in three dimensions. A study integrating 3D clustering with trajectory optimization demonstrated the potential of this approach by authors in [15]. The authors used the A-star algorithm, UAVs were strategically deployed to maximize coverage while adhering to energy and resource constraints. This method proved particularly useful in disaster zones, enabling UAVs to navigate challenging terrains while effectively maintaining optimal connectivity.

Energy-aware clustering models: These remain a critical factor in UAV operations, particularly during prolonged disaster relief missions. The distributed clustering for user devices (DCUD) model addressed this by selecting CHs based on their residual energy levels and proximity to users. This energy-aware approach ensures that UAVs with limited power are not overburdened, thereby extending the overall network lifespan. Such strategies are vital for maintaining consistent communication in resource-constrained environments [16].

Multi-hop clustering and connectivity: In large-scale deployments, multi-hop clustering emerges as a viable solution for expanding coverage and reducing latency. A notable

approach combined device-to-device (D2D) communication with clustering proposed by [17] to create a resilient network architecture. This model allows UAVs to relay data between clusters, ensuring seamless connectivity even in scenarios with limited direct communication links. By reducing the dependency on centralized communication, the method enhanced network scalability and reliability [17].

The roles of predictive analytics as UAV applications evolve and the integration of predictive analytics into clustering frameworks has become increasingly important. By leveraging historical and real-time data, predictive clustering techniques can anticipate mobility patterns and dynamically adjust clusters. This capability is particularly valuable in disaster scenarios in which user density and environmental conditions change rapidly. Such methods have shown promise in maintaining service quality while reducing computational demands proposed by authors in [14,15].

### *2.3. Metaheuristic Algorithms for Disaster Response*

Metaheuristic algorithms have become indispensable for addressing the complexities of disaster response scenarios, particularly when UAVs are employed. These algorithms, known for their capacity to solve non-linear, multi-objective optimization problems, are increasingly used to enhance UAV trajectory planning, resource distribution, and real-time decision-making. Their versatility lies in balancing computational efficiency with adaptability to dynamic environments, making them ideal for high-stake, time-sensitive situations [18–20].

One widely studied algorithm is PSO, inspired by the social behavior of birds and fish. In disaster response, PSO has been employed to optimize UAV path planning by iteratively refining candidate solutions to achieve collision-free navigation. In [19], authors have demonstrated its ability to reduce energy consumption while ensuring effective area coverage. However, PSO often suffers from premature convergence due to its reliance on random oscillations, especially in highly dynamic scenarios, prompting researchers to explore hybrid models that enhance its resilience and precision [19].

The smart flower optimization algorithm (SFOA) offers a refreshing alternative, leveraging the natural growth behavior of flowers to solve optimization challenges. By efficiently managing the exploration and exploitation trade-offs, the SFOA has shown remarkable performance in routing UAVs during pre-disaster assessments and emergency responses. Comparative studies indicate that SFOA outperforms traditional algorithms such as PSO in minimizing transportation costs and achieving faster computational convergence, making it particularly valuable for real-time operations [18]. Similarly, GAs continue to be the cornerstone of UAV optimization research. Known for their iterative selection, crossover, and mutation processes, GAs excel in multi-objective optimization tasks, such as balancing energy consumption, minimizing latency, and maximizing resource distribution. Despite their robustness, their application in disaster scenarios often encounters scalability challenges due to high computational demands, especially when rapid deployment is critical.

Recently, novel algorithms, such as grasshopper optimization (GHO) and the flower pollination algorithm (FPA) proposed by [18,19], have gained attention for their application in UAV path planning. These algorithms emphasize adaptability to obstacles and dynamic conditions and show promising results in simulation studies. However, their practical deployment in large-scale disaster scenarios remains limited, as they require further refinement to reduce the computational overhead [18,19]. Finally, although significant advancements have been made, the next frontier for metaheuristic algorithms lies in improving their scalability and adaptability. Incorporating predictive analytics and real-time data streams into these models enables UAVs to respond more effectively to rapidly changing conditions proposed by [20]. Furthermore, hybrid frameworks that integrate

machine learning and metaheuristics can revolutionize disaster response by making UAV networks more intelligent, efficient, and resilient [20].

#### 2.4. Recent Advances in UAV-Assisted Communication

In recent years, UAV-assisted communication has witnessed remarkable advancements driven by the increasing need for reliable, adaptable, and energy-efficient networks, particularly in disaster scenarios [21–24]. These developments have focused on leveraging cutting-edge learning techniques, innovative energy solutions, and Internet of things integration to overcome the inherent challenges of UAV operations.

The growing convergence of UAV systems with emerging technologies, such as 6G, opens up exciting possibilities. UAVs are expected to be pivotal in enabling ultra-reliable low-latency communication (URLLC) and massive machine-type communication (mMTC) in such networks. A detailed survey of UAV channel modeling highlights key challenges, including the impact of dynamic airframe shadowing, UAV mobility, and fluctuating network conditions. Addressing these issues requires advanced channel-sounding techniques to ensure robust connectivity, particularly in complex disaster environments [23].

At the same time, the authors in [24] have proposed a method for UAVs equipped with energy-harvesting capabilities, which has shown great promise. By harnessing RF energy from ambient signals, UAVs can operate for extended periods without frequent battery replacement. This advancement enhances their utility in prolonged missions and reduces operational costs and environmental impacts. Such systems are particularly well suited for disaster recovery operations, where infrastructure may be damaged or non-existent [24].

IoT integration has revolutionized UAV communication systems, enabling real-time monitoring and rapid emergency response. The authors in [22] have demonstrated how IoT-connected UAVs can collect and process vast amounts of environmental data, such as temperature, humidity, and structural stability, which are critical in post-disaster recovery. These UAV systems act as mobile data hubs, bridging the communication gap in areas where traditional networks are unavailable. Combining UAV mobility with IoT scalability provides a robust framework for handling dynamic and unpredictable disaster scenarios [22]. Energy efficiency remains a central challenge in UAV operations, with limited battery life often constraining functionality. Recent innovations in wireless power transfer (WPT) and energy harvesting (EH) technologies offer potential solutions by authors in [24]. The authors have utilized ambient RF energy where the UAVs can sustain their operations over longer durations, reducing the need for physical battery replacement and maintenance. This capability is particularly critical in disaster-stricken areas, where recharging infrastructure may be sparse. Furthermore, these advancements align with broader sustainability goals by minimizing electronic waste and enhancing operational efficiency [24].

Although UAV-assisted networks have made significant progress, several hurdles remain [22]. The authors have shown that energy constraints still limit the scale of UAV deployment, particularly in large-scale disaster scenarios. Scalability also presents a challenge as UAV networks become increasingly dense and complex. Looking ahead, research must focus on optimizing UAV cooperation and trajectory planning to enable seamless coordination in multi-UAV environments. Additionally, integrating solar power and enhanced energy-harvesting technologies can further extend the operational durations of UAVs and improve their reliability [22]. In summary, advances in UAV-assisted communication have paved the way for more resilient and adaptive disaster response systems. Through the combination of next-generation connectivity, IoT integration, energy-harvesting innovations, and intelligent algorithms, UAV networks have been poised to address future challenges. These systems promise enhanced efficiency and scalability and offer a lifeline in critical disaster scenarios.

### 2.5. Research Gap and Contribution

Despite the significant advancements in UAV-assisted networks, several gaps persist in the existing literature:

1. Integration of mobility prediction with clustering: Most studies fail to incorporate predictive mobility models into clustering algorithms, which are essential for proactive UAV positioning and resource allocation.
2. QoS-aware decision-making: Few approaches consider real-time QoS metrics, such as latency, throughput, and reliability, during UAV deployment and trajectory planning.
3. Dynamic adaptability in disaster environments: Traditional optimization methods often rely on static assumptions or offline training, limiting their ability to adapt to rapidly changing disaster conditions.

This study proposes a hybrid APC-GA framework that combines dynamic clustering with real-time trajectory optimization to address these challenges. The framework ensures scalable and reliable operation across diverse environments by integrating mobility prediction models and QoS-aware decision-making. This approach dynamically adapts to environmental changes, user mobility patterns, and varying communication demands, thereby offering a robust UAV-assisted disaster response solution. A detailed comparison of the related studies is provided in Table 1.

Currently, the available works on UAV path planning performance fall into five broad categories based on user equipment (UE) mobility. The first category focuses on static UE, where trajectories are optimized assuming fixed user locations, often neglecting the impact of user mobility and dynamic environmental conditions (see [7,25–30]). The second category considers quasi-stationary UEs, where users are mostly stationary with occasional minimal movement, making mobility a minor factor in optimization (see [31]). The third category involves random mobility, where user movements are unpredictable, often modeled using stochastic processes, but without considering group or coordinated movement patterns (see [32–34]). The fourth category addresses controlled mobility, where user movements follow predefined or predictable patterns, such as coordinated evacuations or group mobility scenarios (see [35,36]). Finally, the fifth category where this study falls into is the dynamic UE, where user mobility is highly dynamic, requiring real-time adaptation to rapid changes in user distributions and network conditions. However, while works such as [29,37] have some commonalities with this study, such as base station losses, they lack several critical aspects that are addressed here. Specifically, these studies do not consider: (1) swarm UAVs, (2) different QoS requirements, (3) mobility models, and (4) dynamic environments. This work integrates all these dimensions, providing a comprehensive approach for optimizing UAV swarm trajectories in challenging disaster scenarios. This study uniquely addresses the impact of progressive base station losses, ranging from 10% to 90%, to evaluate the resilience and adaptability of UAV swarm path planning. By simulating increasingly severe failures, the necessity of dynamic path optimization is emphasized to restore coverage and maintain QoS compliance, even under extreme infrastructure disruptions. To ensure a fair and consistent comparison, well-established metaheuristic algorithms—GA, PSO, and ACO—were selected as benchmarks. These algorithms were implemented under identical simulation settings, including user mobility models, communication constraints, and base station loss scenarios. This approach ensures that the comparison highlights the unique contributions and effectiveness of the proposed hybrid APC-GA framework. On this basis, the study introduces a comprehensive approach to dynamically adapt UAV swarm trajectories while addressing the challenges of real-time mobility, communication constraints, and severe base station losses.



**Table 1.** Comparison of UAV-BS Deployment Techniques.

Study	UE Mobility Modeled	Types of Mobility	Environment Covered	Mobility Prediction	Trajectory Optimization	Clustering Technique	QoS Awareness	Energy Efficiency
[25]	Static UE	None	Urban	No	PSO-based optimization	K-means	No	Moderate
[7]	Static UE	None	Post-disaster	No	ABC Algorithm	None	No	Low
[31]	Quasi-stationary	Directional	Suburban, Rural	Yes	Proactive UAV adjustments	DBSCAN	Limited	Low
[32]	Random mobility	Random Walk	Disaster zones	No	Behavioral Imitation Learning	None	Yes	Moderate
[35]	Controlled mobility	Directional	Rural	Yes	Optimal transport theory	None	Yes	High
[36]	Controlled mobility	Directional	Urban	Yes	3D trajectory optimization	None	Yes	High
[33]	Random mobility	Random Walk	Urban	Yes	Machine learning-based optimization	None	Yes	Moderate
[26]	Static UE	None	Urban	No	Heuristic placement	None	No	Low
[34]	Random mobility	Random Walk	Urban	No	Heuristic placement	None	No	Low
[27]	Static or Quasi-stationary UE	None	Urban and Suburban	No	A Whale Optimization Algorithm	None	Yes	None
[28]	Static UE	None	Urban	No	Self-organizing architecture	None	No	Moderate
[29]	Static UE	None	Urban	No	Air-ground integrated network	K-means	No	Moderate
[30]	Static UE	None	Urban, Suburban, Dense Urban, High-rise Urban	Yes	Genetic Algorithm-based 3D deployment	K-means	High	Moderate
Proposed Work	Dynamic UE	RWPM, RPGM	Urban, Suburban, Dense Urban, High-Rise Urban	Yes	GA + APC Hybrid for real-time paths	APC	High QoS metrics	High energy optimization for hover and travel

### 3. Environment Modeling

This section outlines the foundational assumptions and design of a system model tailored for UAV swarm deployment in disaster scenarios across diverse environments, including urban, suburban, dense, and high-rise urban settings. The primary goal is to re-establish connectivity for user equipment (UE) affected by natural disasters. Unlike traditional single-mobile aerial base station (MABS) deployments, this model leverages a coordinated UAV swarm to provide scalable and adaptive solutions that meet the specific challenges of different terrains.

The system responds to situations where terrestrial BSs have failed, leaving UEs disconnected. Each UAV in the swarm functions as a mobile aerial base station, collaborating to dynamically adjust positions, trajectories, and altitudes to restore coverage. Figure 2 illustrates the overall system architecture, showing how UAVs interact with different environments to create reliable communication networks. By deploying a swarm rather than relying on a single MABS solution, the system can cover a wider area, adapt to dynamic user mobility, and ensure redundancy in challenging scenarios.

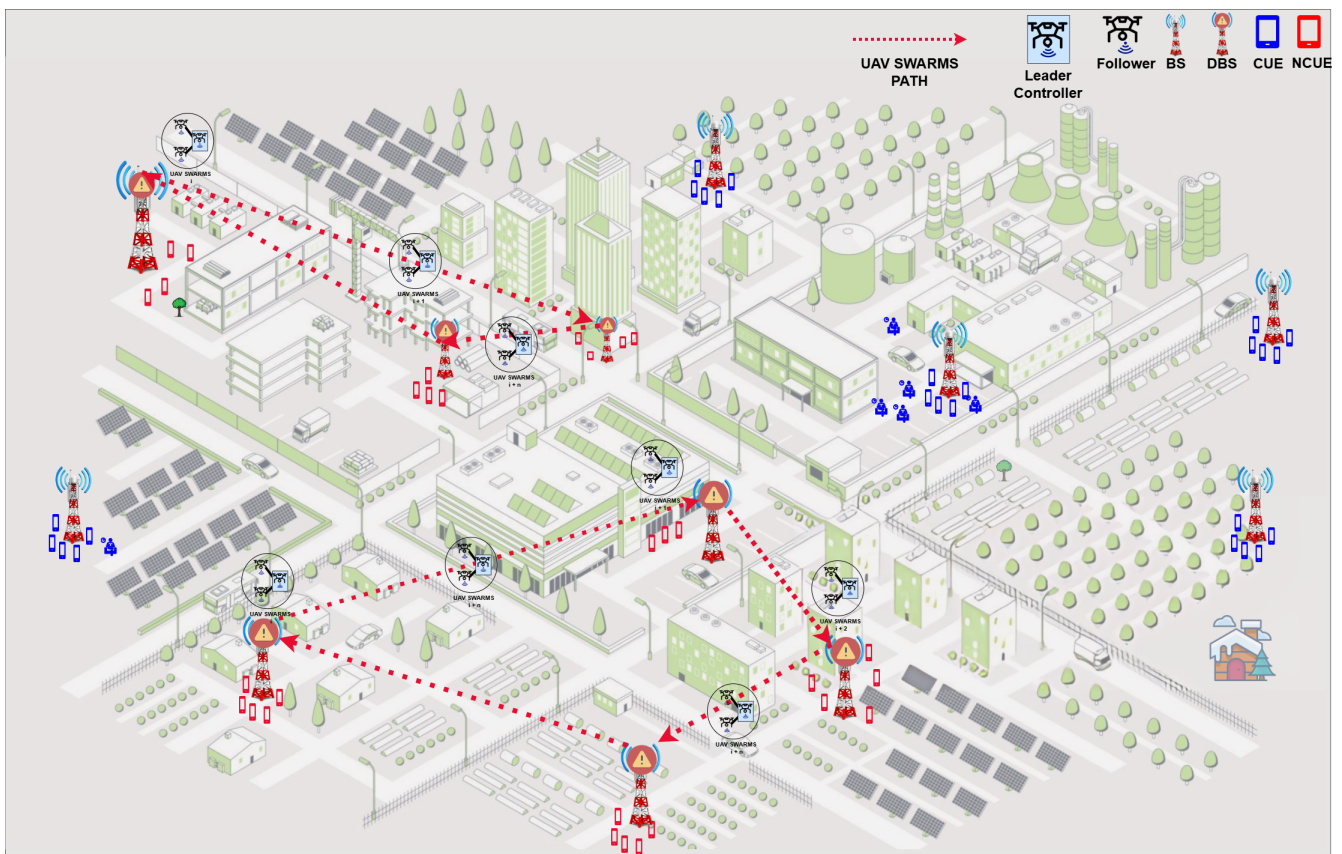


**Figure 2.** Considered environmental setup. Assumed BS circular with radius fails; swarm UAVs are deployed into the same region to provide cellular coverage or for assessment.

One of the distinct features of the system is its adaptability to various environments.

- In urban areas, UAVs navigate through dense building structures, avoiding obstructions and optimizing communication links for effective service delivery.
- In suburban settings, UAVs utilize clustering techniques to distribute coverage efficiently, addressing the broader spacing between UEs.
- For dense urban regions, the swarm handles high UE densities, managing interference and ensuring consistent data rates even in congested zones.

- In high-rise urban environments, the system dynamically adjusts UAV altitudes, enabling vertical coverage for multi-story buildings and skyscrapers.

The affected region was simulated as a 25 km × 25 km area, designed to represent the diversity of real-world disaster zones. This area size was chosen based on the typical scale of medium-sized urban and semi-urban regions affected by natural disasters or large-scale infrastructure failures. Similar approaches to modeling disaster zones have been utilized in UAV network optimization studies, such as [29,37], demonstrating the generality and relevance of this test size.

The Poisson distribution ( $\lambda = 100 \times 25$ ) used for UE distribution reflects the uneven population densities common in such scenarios, while failed base stations ( $\lambda = 10 \times 25$ ) simulate sporadic infrastructure damage. As observed in prior works [29], UAVs are well-suited for reconnections in regions with dispersed or clustered populations, and this setup ensures the test area is representative of real-world disaster scenarios. Red UEs in Figure 2 highlight disconnected users who receive immediate attention from the UAV swarm, whereas blue UEs remain unaffected by the disaster. Isolated UEs benefit from temporary reconnections established through UAV mobility.

This system integrates advanced optimization techniques, including APC, graph theory, and GA, to ensure efficient UAV deployment. These techniques help the swarm dynamically adapt to the real-time distribution of users and environmental challenges, prioritizing energy efficiency, reduced latency, and robust coverage. Overall, this UAV swarm-based model addresses the critical connectivity gaps created by disasters, offering a versatile solution that performs effectively in diverse environments. Its ability to dynamically adapt to changing conditions and prioritize unconnected users highlights its potential as a key enabler of resilient communication networks during emergencies. This is shown in Table 2. The parameters and settings utilized in this simulation framework for UAV swarms were derived and organised based on categories to ensure clarity and comprehensive coverage of various factors influencing performance shown in Table 2. The environment category incorporates parameters such as simulation area, UE distributions, base station (BS) placements, mobility speeds, and environmental scenarios from studies addressing diverse deployment landscapes [29,30]. Environment parameters are specifically calibrated to represent path loss characteristics for different urban and suburban environments [30]. For mobility models, user mobility is characterized through established models such as the random waypoint model (RWPM) and reference point group mobility (RPGM), incorporating speed, variation, and group dynamics [38]. The UAV swarm parameters reflect scalability and optimization, focusing on swarm sizes, capacity, trajectory optimization algorithms, communication ranges, and coordination protocols [29,30,37]. Finally, QoS parameters define data rate requirements for diverse UE demands, and base station failures simulate network resilience under failure scenarios [29,30]. These parameters collectively provide a structured approach to modeling UAV swarm behaviors and evaluating system performance under varied operational conditions.

There are three different data rate requirements that was adopted in this study based on parameters detailed in prior work, particularly the study by [30], where these parameters were tested and validated under diverse UAV deployment environments for all UEs:  $c_1 = 5$  (Mbps),  $c_2 = 2$  Mbps, and  $c_3 = 1$  Mbps, where each UE has one of these three data rate requirements determined to ensure reliable communication, particularly in challenging disaster scenarios. This requirement is set by using the capacity equation (Equation (1)), where  $C_i$  represents the data capacity allocated to UE  $i$ ,  $BW$  denotes the total bandwidth available for communication and  $SINR_i$  denotes the SINR of UE  $i$ . This formulation integrates user-specific quality of service (QoS) requirements ( $R_{QoS,i}$ ) to ensure that all connected users meet or exceed their individual minimum data rate needs.

**Table 2.** Global simulation parameters and settings for UAV swarms [29,30,37,38].

Category	Parameter	Notation/Value	Description
Environment	Simulation Area	$A = 25 \text{ km} \times 25 \text{ km}$	Total area for UE and BS placements.
	UE Distribution ( <i>UED</i> )	$\lambda_{\text{UE}} = \{50, 100, 150, \dots, 450\}$	Number of UEs tested at different densities, incremented by 50, represented as a finite set of Poisson-distributed users.
	BS Distribution	$\lambda_{\text{BS}} = 10 \times 25$	Poisson-distributed BSs.
	UE Mobility Speed	$v_{\text{UE}} \in [0, 20] \text{ m/s}$	Range of UE mobility speeds.
	Environments	$\{E_1, E_2, E_3, E_4\}$	Urban ( $E_1$ ), Suburban ( $E_2$ ), Dense Urban ( $E_3$ ), High-Rise Urban ( $E_4$ ).
Mobility Models	Mobility Model 1	RWPM	Random Waypoint Mobility for individual users.
	Mobility Model 2	RPGM	Reference Point Group Mobility for groups of users.
	UE Speed	$v_{\text{UE}} \in [0, 20] \text{ m/s}$	UE movement speed in both models.
	Path Variation	$P_{\text{var}} = 0.1$	Pause probability for RWPM.
	Group Deviation	$G_{\text{dev}} = 0.5$	Maximum deviation in the RPGM.
	Time Step	$\Delta t = 1 \text{ s}$	Discrete time step for mobility updates.
UAV Swarm Parameters	UAV Swarm	$N \in \{1, 2, 3, \dots, 10\}$	Number of UAVs swarms.
	UAV Capacity	$C_{\text{UE/UAUV}} = 200$	Max UEs per UAV.
	Trajectory Optimization	$\{\text{GA} + \text{APC}, \text{GA}, \text{PSO}, \text{ACO}\}$	Algorithms for swarm path planning.
	Communication Range	$R = 3 \text{ km}$	Max UAV communication range.
	Coordination Protocol	Distributed	Swarm communication strategy.
	Simulation Iterations	17,000	Total number of iterations for simulation optimization algorithms.
QoS Parameters	Data Rate	$\{C_1 = 5 \text{ Mbps}, C_2 = 2 \text{ Mbps}, C_3 = 1 \text{ Mbps}\}$	Different data rate requirements for all UEs.
Base Station Failures	BS Failures	$B \in \{10, 20, \dots, 90\}$	Number of failed base stations considered.
	Failure Distribution	Uniform	Distribution pattern of failed base stations.
	Recovery Priority	Highest UE density	Priority given to areas with the densest unconnected UEs.

The SINR was evaluated using Equation (2), which accounts for the interference and noise in a realistic swarm-based communication environment. The received power ( $P_{\text{Rx},i}$ ) at UE  $i$  is derived from the transmission power of its associated UAV ( $P_{\text{Tx}}$ ), combined with the antenna gains at both the transmitting and receiving ends ( $G_{\text{Tx}}, G_{\text{Rx}}$ ), and is adjusted for path loss ( $PL_i$ ). Interference from neighboring UAVs ( $P_{\text{Int},j}$ ) and environmental noise ( $\eta$ , typically set to  $-112 \text{ dBm}$ ) [39] further influence the SINR values.

For practical scenarios:

- Transmission power levels: The UAV transmission power ( $P_{\text{Tx}}$ ) is configured at 30 dBm to balance coverage and energy efficiency. In comparison, the BSs are assumed to transmit at 46 dBm for a more extensive reach. The UE power is capped at 10 dBm to conserve device energy without sacrificing communication quality.
- Interference management: By incorporating interference from other UAVs, the SINR model reflects realistic swarm dynamics, where overlapping coverage areas may degrade communication quality.
- MIMO configurations: Leveraging multiple-input, multiple-output (MIMO) technology, the system can support simultaneous connections to multiple UEs, enhancing data throughput and spectral efficiency. This is particularly critical in high-density, highly mobile environments.

This refined framework emphasizes adaptability and robustness. The integration of QoS constraints ensures that communication remains reliable and efficient, even under variable conditions such as user mobility, dynamic swarm deployment, or environmental interference. The capacity and SINR models align with the operational challenges of UAV-

assisted networks, addressing both interference mitigation and the necessity for consistent data delivery in disaster recovery scenarios.

The capacity equation incorporates user-specific QoS requirements ( $R_{QoS,i}$ ).

$$C_i = BW \cdot \log_2(1 + \text{SINR}_i), \quad \forall i \in \text{UEs}, \quad C_i \geq R_{QoS,i} \quad (1)$$

The SINR equation includes interference from other UAVs and noise with a swarm-specific interference model:

$$\text{SINR}_i = \frac{P_{R_x,i}}{\sum_{j \neq i} P_{\text{Int},j} + \eta'}, \quad P_{R_x,i} = \frac{P_{T_x} \cdot G_{T_x} \cdot G_{R_x}}{PL_i}, \quad \forall i \in \text{UEs} \quad (2)$$

The Okamura–Hata propagation path loss (PL) model, widely recognized for its reliability in modeling signal attenuation, was employed in this study to provide an approximate representation of general disaster scenarios. This model was chosen for its capability to effectively simulate urban and suburban environments while accounting for critical factors such as frequency, height, and distance.

For this implementation, the carrier frequency was set to 700 MHz, aligned with LTE Band 14 [40], which is frequently designated for public safety and disaster response applications. This frequency choice ensures robust signal penetration and minimal interference in challenging environments.

The primary path-loss calculation is expressed in Equation (3), which integrates distance-based logarithmic attenuation and environment-specific adjustments. The constants  $A$  and  $B$  detailed in Equations (4) and (5), respectively, encapsulate the effects of frequency, base station height, and UE height. These equations incorporate empirically derived coefficients to accurately reflect the signal behavior under varying conditions.

This approach offers a balanced trade-off between model simplicity and predictive accuracy, making it well suited for UAV swarm deployment in disaster scenarios. By leveraging the Okamura–Hata model, this study ensures that the propagation characteristics are realistic and applicable to diverse terrain types and urban densities.

### 3.1. Path Loss Modeling

Accurate path-loss modeling is essential for UAV swarm-assisted communication systems because it directly affects the quality of signal reception and overall system performance. The updated equations integrate the dynamic environmental parameters and user mobility.

#### 3.1.1. General Path Loss Model

The path loss ( $PL$ ) between a UAV and a user is represented as

$$PL = A + B \cdot \log_{10}(d) + \eta_{\text{Env}} \quad (3)$$

where:

- $d$ : Distance between the UAV and UE, measured in meters.
- $\eta_{\text{Env}}$ : Environment-specific attenuation, which accounts for urban, suburban, dense urban, and high-rise urban conditions.

#### 3.1.2. Calculation of Parameter $A$

Parameter  $A$  encapsulates the effects of frequency, UAV altitude, and user device height:

$$A = 69.55 + 26.16 \cdot \log_{10}(f) - 13.82 \cdot \log_{10}(h_b) - a(h_m) \quad (4)$$

Here:

- $f$ : Carrier frequency (MHz) (e.g., 700 MHz for LTE Band 14).
- $h_b$ : UAV altitude in meters.
- $a(h_m)$ : A correction factor based on the height of the UE ( $h_m$ ).

The correction factor  $a(h_m)$  is further refined for the disaster scenarios as follows:

$$a(h_m) = (1.1 \cdot \log_{10}(f) - 0.7) \cdot h_m - (1.56 \cdot \log_{10}(f) - 0.8) \quad (5)$$

### 3.1.3. Calculation of Parameter $B$

The parameter  $B$  accounts for variations in UAV altitude and is given by

$$B = 44.9 - 6.55 \cdot \log_{10}(h_b) \quad (6)$$

In the context of (4) for this disaster recovery scenario, the function  $a(h_m)$  represents the impact of UE height,  $h_m$ , on the overall signal propagation and loss dynamics. The parameter  $f$  denotes the carrier frequency in hertz, and  $\log(f)$  reflects the logarithmic impact of frequency on the signal behavior. Constants 1.1, 0.7, 1.56, and 0.8 are coefficients that are carefully calibrated to capture the nuanced effects of frequency scaling and height in disaster-affected communication environments. These coefficients ensure that the model aligns with the realistic propagation characteristics observed in the post-disaster scenarios.

Equation (5) serves as a key component for adapting the signal model to different scenarios by integrating parameters, such as user height and operating frequency, to fine-tune the path loss calculations. This approach provides a more accurate representation of the challenges faced in delivering reliable communication services in environments with diverse terrains, building heights, and user distributions.

Equation (8) further characterizes the environmental impact, which dynamically adjusts the model based on environmental conditions such as urban density, LOS availability, and potential obstructions. In cases where the environmental variable is negligible or controlled (e.g., uniform terrain), the equation is simplified by setting the environmental contribution to zero, ensuring computational efficiency without sacrificing the model accuracy [41].

This dual-layer modeling of  $a(h_m)$  and  $Env$  provides a comprehensive framework for assessing signal behavior, enabling tailored responses to UAV swarms in disaster-stricken regions. The flexibility of these equations makes them applicable to various deployment environments, thereby ensuring robust communication under diverse conditions.

$$a(h_m) = ((\alpha_{env} \cdot \log_{10}(f) - \beta_{env}) \cdot h_m) - ((\gamma_{env} \cdot \log_{10}(f) - \delta_{env})) \quad (7)$$

where:

- $\alpha_{env}, \beta_{env}, \gamma_{env}, \delta_{env}$ : Environment-specific coefficients for urban, suburban, dense urban, and high-rise urban environments.
- $f$ : Carrier frequency ( MHz).
- $h_m$ : UE height (in meters).

$$Env = \begin{cases} \eta_{LOS} & \text{if LOS,} \\ \eta_{NLOS} & \text{if NLOS.} \end{cases} \quad (8)$$

where:

- $\eta_{LOS}$ : Environment-specific attenuation for LOS conditions.
- $\eta_{NLOS}$ : Environment-specific attenuation for non-line-of-sight (NLOS) conditions.

Equation (7): Correction factor  $a(h_m)$  is an environment-specific propagation characteristic. This ensures a better accuracy across diverse terrains and varying frequencies. The coefficients  $\alpha_{env}, \beta_{env}, \gamma_{env}, \delta_{env}$  allow for precise modeling of the path loss based on the terrain type.

Equation (8): The environmental factor ( $Env$ ) accounts for LOS and NLOS conditions. This dynamic adjustment ensures that the UAV swarm deployments remain robust across all four environments, thereby compensating for the differences in signal propagation.

The UAV swarm units operating collectively are maintained at a uniform cruising speed of 50 km/h to ensure consistent deployment and response efficiency [29]. This speed was chosen as it represents a practical balance between rapid deployment that enables UAVs to respond promptly to dynamic scenarios, such as disaster zones or network coverage gaps [29,37]. Speeds lower than 50 km/h (e.g., 10 km/h, 20 km/h) were deemed less suitable for urgent deployments, while higher speeds could introduce potential communication instability. Although influential in real-world scenarios, environmental variables, such as wind velocity, precipitation, and other natural factors, were not explicitly modeled in this study to focus on communication performance metrics. Similarly, potential disruptions from wildlife interactions were not factored into the simulation framework, thereby simplifying the analysis.

The affected UE in disaster-impacted regions are organised into clusters using the APC algorithm [42]. This clustering approach dynamically identifies representative cluster centres based on pairwise similarity and effectively minimizes intracluster distances. A damping factor of 0.6 is applied to stabilize the convergence process, enhancing the robustness of the algorithm against fluctuations in the UE distribution.

The spatial distribution of UEs follows an incremental Poisson process to reflect realistic density variations. BS outages were simulated with varying degrees of severity, ranging from 10% to 90% coverage loss. This approach enables a comprehensive analysis of the UAV swarm adaptability under diverse failure scenarios. For example, Figure 3 illustrates an environment in which 30% of BSs are inoperable, leaving UEs in critical need for coverage.

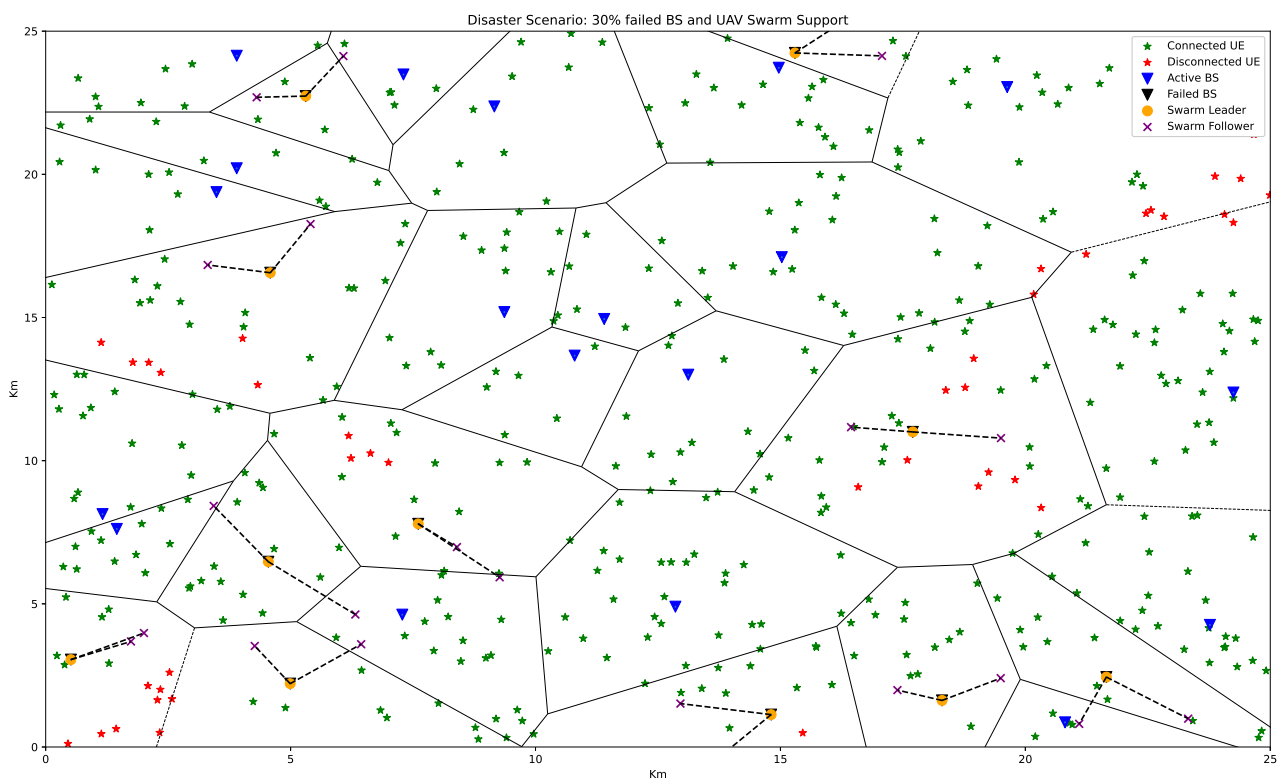


**Figure 3.** Distribution of UEs in the environment. In this example, there is a 30 per cent rate of base station outage.

This modeling approach ensures that UAV swarm deployment strategies are evaluated under realistic, yet controlled conditions, emphasizing their ability to restore connectivity in disaster-stricken regions. The flexibility of the framework accommodates variations in UE density and mobility, thereby providing a robust foundation for optimizing UAV-assisted communication networks.

In this framework, in Figure 3, a UE with active service is represented by blue asterisks, whereas UEs without service, typically affected by base station outages, are indicated by red asterisks. The spatial arrangement of UEs is visualised through Voronoi cells, which define the boundaries of clusters based on their proximity to UAVs or base stations. Active base stations are depicted as blue downward triangles, whereas base stations rendered inoperative because of disaster conditions are marked with black downward triangles.

The simulation encompassed a total area of 25 km<sup>2</sup>, representing a realistic, disaster-stricken environment. Within this setup, each swarm of UAVs, coordinated by a leader drone and supported by follower drones, provides temporary communication coverage to unconnected UEs within their designated clusters. Once the immediate communication needs of a cluster are addressed, the UAV swarm progresses to the next identified centroid, thereby ensuring continuous service restoration across the affected area. This dynamic and adaptive strategy ensures that critical communication links are maintained, even under severe network disruptions in Equation (9).

$$P_{\text{out}} = 1 - \prod_{i=1}^{N_{\text{UE}}} (1 - P_{\text{BS}} \cdot \psi_{\text{env},i} \cdot \chi_{\text{mob},i}) \quad (9)$$

Here,  $P_{\text{out}}$  is the probability of a UE experiencing an outage,  $P_{\text{BS}}$  is the probability of a base station (BS) failing, and  $\psi_{\text{env},i}$  is an environment-specific reliability factor for user  $i$ , defined as

$$\psi_{\text{env},i} = \begin{cases} \eta_{\text{LOS}}, & \text{if LOS,} \\ \eta_{\text{NLOS}}, & \text{if NLOS.} \end{cases} \quad (10)$$

Here,  $\eta_{\text{LOS}}$  and  $\eta_{\text{NLOS}}$  are the environment-dependent attenuation factors, as described in Equation (10).  $\chi_{\text{mob},i}$  is the mobility reliability factor for user  $i$ , which reflects the likelihood of maintaining connectivity during motion. This depends on the mobility model used.

- Random Waypoint Mobility:

$$\chi_{\text{mob},i} = 1 - \frac{\Delta d}{R} \quad (11)$$

where  $\Delta d$  is the distance travelled by the UE once and step  $R$  is the UAV's communication range.

- Reference Point Group Mobility:

$$\chi_{\text{mob},i} = \exp(-\delta_g \cdot \frac{\Delta d}{R}) \quad (12)$$

where  $\delta_g$  denotes the group-specific deviation factor.

This equation comprehensively represents the outage probability, considering the environmental and mobility effects specific to UAV swarm deployment in disaster response scenarios.

### 3.2. Problem Definition

To model UAV swarm deployment effectively, the problem is framed as a data allocation and coverage optimization task, ensuring that the maximum number of users (UEs) is served while adhering to various constraints. UAVs act as temporary aerial base stations



(UAV-BSs) and are responsible for delivering a sufficient data rate to each UE, based on their unique requirements. For simplicity, it was assumed that the data rate provided to each UE matched the requested rate. This transforms the data allocation problem into a combinatorial optimization problem, which is often recognised as NP-hard owing to its complexity [43]. The objective is expressed as

$$\max_{R_j, m_j} \sum_{j=1}^{|Q|} \sum_{i=1}^{|P|} \gamma_{ij} \quad (13)$$

where  $\gamma_{ij}$  is a binary variable representing whether the UAV-BS  $j$  serves user  $i$ ,  $|P|$  is the set of UEs, and  $|Q|$  is the set of UAV-BSs. This optimization is subject to the following constraints:

$C_1$ : This ensures that the UE is served only by the UAV-BS if it falls within its coverage radius.

$$\|m_j - \gamma_{ij}u_i\| \leq R_j + M(1 - \gamma_{ij}), \quad i \in \{1, 2, \dots, |P|\}, j \in \{1, 2, \dots, |Q|\}, \gamma_{ij} \in \{0, 1\}.$$

Here,  $m_j$  and  $u_i$  are the positions of the UAV-BS and UE, respectively, and  $R_j$  denotes the coverage radius of the UAV-BS  $j$ . Parameter  $M$  acts as a large constant to handle binary conditions, ensuring that this constraint is only enforced when  $\gamma_{ij} = 1$ .

$C_2$ : This ensures that each swarm UAV does not exceed its maximum data capacity when serving multiple UEs.

$$\sum_{i=1}^{|P|} c_i \gamma_{ij} \leq C_j, \quad j \in \{1, 2, \dots, |Q|\}.$$

Here,  $c_i$  represents the data rate demand of UE  $i$ , and  $C_j$  is the maximum capacity of UAV-BS  $j$ .

$C_3$ : Each UE should be served by a maximum of one UAV-BS.

$$\sum_{j=1}^{|Q|} \gamma_{ij} \leq 1, \quad i \in \{1, 2, \dots, |P|\}.$$

This constraint prevents the UEs from being redundantly served by multiple UAV-BSs.

$C_4$ : The coverage radius of each UAV-BS should not exceed the predefined maximum.

$$R_j \leq R_{\max}, \quad j \in \{1, 2, \dots, |Q|\}.$$

The objective function aims to maximize the number of UEs served by UAV-BSs while adhering to the coverage, capacity, and connectivity constraints. Constraint  $C_1$  ensures that a UAV-BS can only serve a UEs within its communication range. Constraint  $C_2$  enforces capacity limitations, ensuring that UAVs do not exceed their maximum data-handling capabilities. Constraint  $C_3$  guarantees that each UE is connected to at most one UAV-BS, avoiding overlaps and inefficiencies in resource allocation. Finally,  $C_4$  ensures that UAV-BSs operate within their designated coverage limits.

This problem formulation provides a structured approach for addressing the challenge of UAV swarm deployment in disaster scenarios. The constraints balance maximizing service coverage, maintaining QoS, and adhering to operational limitations such as capacity and coverage radius. Considering these constraints, this model facilitates the efficient allocation of UAV-BS resources, ensuring that disconnected UEs are reconnected with minimal

service disruption. Unlike traditional fixed base stations, UAV-BSs offer flexibility and adaptability, making them ideal for rapid deployment in dynamic disaster environments.

$$\min \sum_{i=1}^n \sum_{j=1}^m \sum_{u=1}^{N_{\text{swarm}}} (C_{ij} \cdot X_{iju} + \lambda \cdot E_u) \quad (14)$$

This cost function minimizes the total communication cost  $C_{ij}$  between the UAV  $i$  and UE  $j$  along with the energy consumption  $E_u$  of the UAV  $u$  in the swarm weighted by  $\lambda$  in Equation (14).

$$\sum_{j \in V(k,j)} S_k \cdot X_{iju} \leq C_u, \quad \forall u \in \text{UAV swarm} \quad (15)$$

This constraint in Equation (15) ensures that the service demand  $S_k$  of all UEs assigned to a UAV  $u$  does not exceed its capacity  $C_u$ .

$$\sum_{u=1}^{N_{\text{swarm}}} \sum_{j \in V} \text{Distance}(u, j) \cdot X_{iju} \leq \text{MaxDistance}, \quad \forall u \in \text{UAV swarm} \quad (16)$$

This trajectory optimization minimizes the travel distance for all UAVs in the swarm, while ensuring that it does not exceed the defined maximum distance threshold in Equation (14).

$$\sum_{j=1}^m X_{iju} \geq 1, \quad \forall i \in \text{UEs} \quad (17)$$

The MTSP is adapted to reflect the UAV swarm deployment strategy outlined in Equation (16), where each UE  $i$  must be served by at least one UAV in the swarm to ensure the full coverage of the affected area. Each swarm path must include at least one leader UAV from the assigned swarm in order to ensure seamless coordination and connectivity. This adaptation emphasizes swarm-based UAV networks, where each swarm comprises one leader drone and two follower drones that work in tandem to provide enhanced coverage and connectivity. UAVs in the swarm operate autonomously without human intervention, facilitating rapid deployment in disaster scenarios. The optimization framework expressed in Equation (12) is designed to minimize the total cost by optimizing the allocation of UAVs to mobile user clusters and calculating their trajectories. This formulation accounts for both the leader-follower hierarchy within the swarm and the dynamic mobility patterns of the UE. By integrating these elements, the revised MTSP model addresses the complex requirements of swarm-based UAV operation in diverse and dynamic environments. It ensures robust service delivery by balancing energy efficiency, communication quality, and resource utilization, while meeting the QoS demands of mobile UEs across multiple clusters. This approach builds a scalable and adaptive foundation for UAV swarm deployment in various disaster scenarios.

$$\min \sum_{i=1}^n \sum_{j=1}^m \sum_{u=1}^{N_{\text{swarm}}} (C_{ij} \cdot X_{iju} + \lambda \cdot E_u + \beta \cdot \text{Latency}_{ij}) \quad (18)$$

The number of UAV swarm mission members, represented by  $N_{\text{UAV}}$ , encompasses both the leader and follower drones within each swarm. Each swarm operates cohesively with its trajectory denoted by  $X_{iju}$ , where  $i$  represents the user cluster,  $j$  indicates the specific path segment, and  $u$  denotes the UAV swarm assigned to cluster (16). This parameter is pivotal in determining the spatial and temporal deployment of UAV swarms across disaster-stricken areas.

The capacity requirement for each cluster, denoted by  $C_{ij}$ , defines the communication load that a UAV swarm must handle. Trajectory  $X_{iju}$  is tailored to ensure seamless commu-

nication, considering both the dynamic mobility of UEs and the hierarchical roles of the leader and follower UAVs within each swarm. Unlike traditional MABS-based approaches, this model incorporates swarm-specific dynamics, allowing flexible and efficient coverage in highly dynamic and unpredictable environments.

Short-duration communication bursts are critical in this setup, enabling the UEs to connect to the UAV swarm for intermittent essential data exchanges. These bursts were optimized to maximize coverage and minimize energy expenditure. Unlike the static constraints in Equations (9)–(11), the swarm-based approach dynamically adapts paths and communication patterns based on real-time UE mobility and environmental conditions.

The trajectory planning process for each swarm is rooted in multipath optimization, ensuring that each route traversable by a UAV swarm maintains connectivity while minimizing travel distance. The planning process accommodates multiple potential entry points in the disaster zone, because there is no predefined starting point for the operation of a UAV swarm. The total number of possible edges within this framework is calculated using Equation (17), which offers a combinatorial representation of the swarm UAV routing possibilities. This formulation ensures scalability and adaptability, which are critical for addressing the diverse challenges of disaster response scenarios.

$$\text{total}(E) = \frac{N_{\text{UAV}}!}{(N_{\text{UAV}} - 2)! \cdot 2!} = \binom{N_{\text{UAV}}}{2} = \frac{N_{\text{UAV}} \cdot (N_{\text{UAV}} - 1)}{2} \quad (19)$$

### 3.3. Parameter Settings

Table 2 outlines the global simulation parameters and configurations used to evaluate the performance of the UAV swarm in the studied disaster response environment. The table provides detailed specifications of the simulation setup, including the UAV swarm parameters, QoS constraints, and base station failure scenarios. These parameters serve as the foundation for assessing the scalability, adaptability, and reliability of networks under various operational conditions. The spatial domain ( $A$ ) spans a square area of 25 km  $\times$  25 km, selected to represent the size of medium-scale disaster zones commonly encountered in real-world scenarios, such as floods or earthquakes. This size ensures sufficient coverage for analyzing UAV swarm performance under realistic operational conditions, as supported by similar studies [29,30].

The UE density, denoted by  $\lambda_{\text{UE}}$ , varied incrementally from 50 to 450, following a Poisson distribution. The Poisson distribution was chosen as it accurately models the stochastic nature of user distributions in disaster scenarios, where users are unevenly clustered due to shelter locations or evacuation routes [30]. This approach captures the variability and randomness of real-world user densities.

The mobility of the UEs is introduced as a critical factor, with speeds ranging between 0 and 20 m/s to represent a wide spectrum of movement patterns. Stationary users represent individuals in shelters or static zones, while speeds up to 20 m/s capture vehicular mobility observed during evacuations or dynamic environments [37]. These mobility speeds are reflective of real-world disaster scenarios and ensure robust evaluation across varying user behaviors. Two mobility models, the RWPM and RPGM, were employed to simulate individual and group-based user movements, respectively. RWPM models the independent and random movement of users, while RPGM reflects coordinated group mobility, such as that seen in evacuation convoys or community-based recovery operations. These models collectively provide a comprehensive framework to evaluate UAV swarm adaptability under different mobility patterns [38]. The UAV swarm configurations included swarm sizes ( $N$ ) of (1, 2, 3  $\dots$ , 10) swarms. These sizes were selected to evaluate scalability and performance in varying disaster scenarios: **small swarms** represent localized disruptions or low-density user environments; **medium swarms** reflect typical disaster response scenarios

where moderate coverage and coordination are required; and **large swarms** simulate large-scale disasters requiring extensive coverage and coordination [29].

Each UAV is capable of serving up to 200 UEs ( $C_{UE/UAV}$ ), based on the typical load-handling capacity of UAVs in real-world applications [30]. UAVs operate within a communication range ( $R$ ) of 3 km, which represents a practical range for maintaining stable connections, while ensuring effective coverage restoration [39]. Trajectory optimization algorithms, including GA + APC, GA, PSO, and ACO, were employed to maximize coverage restoration. These algorithms have been extensively validated in UAV network optimization studies and are well-suited for addressing the challenges of dynamic disaster environments [38]. A distributed coordination protocol was implemented to enable seamless inter-UAV communication, ensuring effective collaboration among swarm members. This protocol enhances the swarm's ability to dynamically adapt to varying user densities and coverage requirements. The simulation iterations were set to 17,000 in this study, a parameter adopted from [30] to ensure convergence and robust optimization for the proposed swarm UAV deployment strategy. The higher iteration count allows the metaheuristic algorithms, such as the proposed GA + APC to explore the solution space adequately and achieve reliable convergence.

To maintain stringent QoS requirements, the network adheres to three different data rate requirements for all UEs:  $c_1 = 5$  Mbps,  $c_2 = 2$  Mbps, and  $c_3 = 1$  Mbps. These thresholds were chosen to represent a range of application requirements, from high-bandwidth tasks such as video streaming ( $c_1$ ) to essential communication services such as voice calls ( $c_3$ ) [29,30]. These constraints are critical for ensuring reliable communication in disaster-stricken areas with a high user density and mobility. Base station failures ( $B$ ) were simulated at varying levels ranging from 10% to 90% using uniform distribution patterns. This range reflects real-world disaster scenarios, from localized outages to widespread infrastructure failures [37]. Recovery prioritization is based on UE density, ensuring that areas with the highest concentration of unconnected users are addressed first, which mirrors disaster response strategies in practice. This robust and multifaceted parameterization provides a realistic and comprehensive evaluation framework, enabling the UAV swarm network to be optimized for disaster recovery scenarios that involve dynamic user mobility, varying environmental conditions, and stringent communication requirements. The implementation of the proposed GA + APC algorithm was conducted using Python. The simulations were performed on a system equipped with a 2.4 GHz Intel Core i7-7600U CPU, 64 GB of RAM, and an NVIDIA T1000 (4 GB) graphics card. This hardware configuration was selected to ensure computational efficiency for managing the complex optimization tasks and large-scale disaster scenarios simulated in this study. The operating environment was configured to execute multiple iterations of the algorithm under varying conditions, facilitating a comprehensive evaluation of its performance.

## 4. Proposed Optimal Path Planning for UAV Swarms

### 4.1. Integration of Proposed Fitness Function and Swarm Mutation Strategies

This subsection elaborates on the design of the swarm-GA, which utilizes evolutionary principles to derive optimal solutions for complex scenarios. The algorithm builds on the natural concepts of evolution using mutation and crossover to iteratively explore and refine solutions. These operations enable the swarm to adapt dynamically to changing conditions, thereby ensuring robust and efficient path planning.

The swarm-GA operates by treating each potential solution as a chromosome with adjustable parameters corresponding to the requirements of the problem. Fitness evaluation is central to measuring the suitability of each chromosome for meeting performance criteria, such as service coverage, path efficiency, and QoS compliance. During this evaluation,

UE clusters were formed using APC, a non-supervised method tailored for scenarios with spatially dispersed UEs. Unlike traditional k-means clustering, APC dynamically selects cluster representatives based on similarity metrics, ensuring that the clusters align with the spatial density of the UEs.

Algorithm 1 outlines the foundational steps for initializing a swarm of UAVs and clustering UE in the studied dynamic environment. It employs a structured approach to assign roles to UAVs, cluster UEs using APC, and compute the initial task allocations for the UAV swarm.

---

**Algorithm 1:** Swarm initialization and UE clustering

---

**Data:**  $N_{\text{UAV}}$ : Number of UAVs,  $\lambda_{\text{UE}}$ : UE distribution,  $v_{\text{UE}}$ : UE mobility speed,  $M$ : Mobility model,  $E$ : Environment parameters.

**Result:** Cluster assignments  $V$ , initial paths  $X_{\text{init}}$ .

**Step 1: Swarm Role Assignment**

Define swarm UAV roles:

$$\text{UAV}_{\text{leader}} \rightarrow 1, \quad \text{UAV}_{\text{follower}} \rightarrow N_{\text{UAV}} - 1, \quad \text{UAV}_{\text{coordinator}} \rightarrow 1.$$

**Step 2: UE Initialization**

Initialize the UE positions:

$$P_{\text{UE}} = \{(x_1, y_1), (x_2, y_2), \dots, (x_n, y_n)\}, \quad n = |\lambda_{\text{UE}}|$$

Mobility model  $M$  is applied to compute the UE movement:

$$P_{\text{UE}}(t) = P_{\text{UE}}(t-1) + v_{\text{UE}} \cdot \Delta t.$$

**Step 3: UE Clustering using APC**

Compute the cluster centres  $V = \{v_1, v_2, \dots, v_k\}$ .

$$v_i = \arg \min_j \sum_{j \in P_{\text{UE}}} \text{sim}(j, v_i)$$

where  $\text{sim}(j, v_i)$  denotes the similarity measure for the APC.

**Step 4: Path Initialization**

Assign tasks to UAVs from cluster centre  $V$ .

$$X_{\text{init}} = \{x_1, x_2, \dots, x_{N_{\text{UAV}}}\}, \quad x_u = \{v_i\}_{i \in V}, \quad \forall u \in N_{\text{UAV}}.$$

**Step 5: Cluster Re-Evaluation and Mobility Integration**

Update the cluster centres  $V$  dynamically if the UE positions change.

$$v_i(t) = \arg \min_{j \in P_{\text{UE}}(t)} \text{sim}(j, v_i(t)).$$

Recompute paths  $X_{\text{init}}$  for all UAVs.

$$x_u(t) = \{v_i(t)\}_{i \in V}$$

**Step 6: Output Results**

**return**  $V, X_{\text{init}}$ .

---

The first step in the algorithm defines the distinct roles of the UAVs in the swarm. Each swarm consists of one leader UAV ( $\text{UAV}_{\text{leader}}$ ) responsible for overall coordination, multiple

follower UAVs ( $UAV_{\text{follower}}$ ) executing tasks, and one coordinator UAV ( $UAV_{\text{coordinator}}$ ) to manage communication between UAVs. For a swarm with  $N_{\text{UAV}}$  UAVs,

$$UAV_{\text{leader}} = 1, \quad UAV_{\text{follower}} = N_{\text{UAV}} - 1, \quad UAV_{\text{coordinator}} = 1 \quad (20)$$

This role-based structure ensures an efficient task distribution and coordination. In the next step, UE initialization, the UE positions are initialized as coordinates.

$$P_{\text{UE}} = \{(x_1, y_1), (x_2, y_2), \dots, (x_n, y_n)\}, \quad n = |\lambda_{\text{UE}}| \quad (21)$$

where  $|\lambda_{\text{UE}}|$  represents the total number of UEs in the environment. These initial positions are updated over time based on the mobility model  $M$ , simulating UE movement:

$$P_{\text{UE}}(t) = P_{\text{UE}}(t-1) + v_{\text{UE}} \cdot \Delta \quad (22)$$

where  $v_{\text{UE}}$  is the UE mobility speed and  $\Delta t$  is the time interval. This dynamic adjustment captures real-time changes in the UE locations. In Step 3, UE Clustering using APC is employed to group the UEs into clusters. Each cluster is defined by its centroid  $v_i$ , which minimizes the similarity metric,

$$v_i = \arg \min_{j \in P_{\text{UE}}} \sum_{j \in P_{\text{UE}}} \text{sim}(j, v_i) \quad (23)$$

where  $\text{sim}(j, v_i)$  measures the similarity between a UE  $j$  and cluster centre  $v_i$ . APC dynamically determines the number of clusters and their centroids based on UE density and spatial distribution. These centroids serve as target points for UAV task allocation.

After determining the cluster centres  $V = \{v_1, v_2, \dots, v_k\}$ , the next step is path initialization, in which the initial paths for the UAVs are assigned. Each UAV  $u$  is allocated a set of cluster centres as tasks.

$$X_{\text{init}} = \{x_1, x_2, \dots, x_{N_{\text{UAV}}}\}, \quad x_u = \{v_i\}_{i \in V}, \quad \forall u \in N_{\text{UAV}} \quad (24)$$

This step ensures that each UAV has a predefined route based on the initial UE clustering. Then, in the cluster re-evaluation and mobility integration step, which adapts to changes in UE positions, the algorithm dynamically updates the cluster centroids:

$$v_i(t) = \arg \min_{j \in P_{\text{UE}}(t)} \text{sim}(j, v_i(t)) \quad (25)$$

This recalibration ensured that the clusters remained relevant as the UEs moved. Correspondingly, the UAV paths are computed as follows:

$$x_u(t) = \{v_i(t)\}_{i \in V} \quad (26)$$

This real-time adjustment integrates UE mobility into UAV task planning, enabling the swarm to maintain an efficient coverage and service. Finally, the algorithm outputs the updated cluster assignments  $V$  and initial paths  $X_{\text{init}}$ , which serve as the basis for subsequent optimization steps.

$$\text{Output: } V, X_{\text{init}} \quad (27)$$

This algorithm provides a robust framework for initializing UAV swarm operations in dynamic environments. By integrating mobility models and clustering techniques, UAVs can efficiently adapt to changes in the UE distribution while maintaining effective task allocation and coordination.

Algorithm 2 outlines a genetic optimization approach for UAV path planning and task allocation, focusing on achieving efficient resource utilization while satisfying the QoS requirements. The process begins with the initialization of paths  $X$  from the provided  $X_{\text{init}}$ , which represents the initial allocation of tasks and paths for all the UAVs in the swarm. The fitness of each path was computed using a comprehensive function designed to balance the path length, and QoS metrics.

The fitness function is defined as

$$\mathcal{F}(X) = \sum_{u=1}^{N_{\text{UAV}}} \left( \frac{1}{L(X_u)} + \frac{\text{QoS}_{\text{satisfied}}}{\text{QoS}_{\text{total}}} - \frac{E_{\text{cost}}(X_u)}{E_{\text{max}}} \right) \quad (28)$$

where  $L(X_u)$  is the length of the path assigned to the UAV  $u$ ,  $\text{QoS}_{\text{satisfied}}$  measures the proportion of the QoS constraints satisfied, and  $E_{\text{cost}}(X_u)$  quantifies the energy consumption of the UAV along the path relative to its maximum energy capacity  $E_{\text{max}}$ . The fitness function ensures that shorter paths, higher QoS satisfaction, and lower energy costs are achieved.

The initial fitness of each chromosome (path configuration) was evaluated by calculating the QoS satisfaction and ensuring compliance with SINR requirements. The SINR for UE  $i$  is computed as

$$\text{SINR}_i = \frac{P_{\text{Tx}}}{\sum_{j \neq i} P_{\text{Int},j} + \eta} \quad (29)$$

where  $P_{\text{Tx}}$  is the transmitted power,  $P_{\text{Int},j}$  represents the interference from the other UAVs, and  $\eta$  is the noise power. QoS satisfaction, denoted  $\text{QoS}_{\text{satisfied}}$ , is calculated as the sum of the users meeting the SINR threshold  $\text{SINR}_{\text{min}}$ :

$$\text{QoS}_{\text{satisfied}} = \sum_{i=1}^{N_{\text{UE}}} \mathcal{I}(\text{SINR}_i \geq \text{SINR}_{\text{min}}) \quad (30)$$

where  $\mathcal{I}$  denotes an indicator function. The genetic algorithm iteratively refines the population of paths using mutation operators to explore the solution space and enhance fitness. These operations were divided into two categories.

In chromosome mutators, section swapping reorders segments within a UAV's path  $x_u$ , enabling more efficient task sequencing. Point insertion adjusts the position of tasks within a path to minimize travel and hovering costs, computed as

$$\text{Cost}(x_u) = \sum_{i=1}^k (d_{i,u} + P_{\text{hover}} \cdot t_{\text{hover}}) \quad (31)$$

where  $d_{i,u}$  is the distance travelled,  $P_{\text{hover}}$  is the hovering power, and  $t_{\text{hover}}$  is the time spent on hovering.

Cross-chromosome mutators comprise task swapping, which transfers tasks between UAVs  $x_u$  and  $x_v$ , balancing their workloads. The joint mutator then combines paths to optimize coordination among the leader UAVs. The separation mutator Splits the paths to distribute tasks among multiple UAVs more effectively. These mutation operators ensure that the solution space is thoroughly explored, thereby preventing the premature convergence to suboptimal paths. After applying mutations, the paths are updated and their fitness is computed. This step involves recalculating  $\mathcal{F}(X)$  for all chromosomes and incorporating the effects of the updated paths, SINR compliance, and energy constraints, as shown in Equation (28).

**Algorithm 2:** Path optimization and task allocation

**Data:**  $V$ : Cluster assignments,  $X_{\text{init}}$ : Initial paths, QoS constraints,  $C_{\text{UAV}}$ : UAV capacity,  $\text{SINR}_{\text{min}}$ : Minimum SINR, Mutation Operators.

**Result:** Optimized paths  $X^*$ .

**Step 1: Initialize Optimization Framework**

Set the initial paths  $X \leftarrow X_{\text{init}}$ ;

The fitness function  $\mathcal{F}(X)$  is defined as

$$\mathcal{F}(X) = \sum_{u=1}^{N_{\text{UAV}}} \left( \frac{1}{L(X_u)} + \frac{\text{QoS}_{\text{satisfied}}}{\text{QoS}_{\text{total}}} - \frac{E_{\text{cost}}(X_u)}{E_{\text{max}}} \right)$$

where  $L(X_u)$  is the path length and  $E_{\text{cost}}(X_u)$  is the energy consumed by the UAV  $u$ .

**Step 2: Evaluate Initial Fitness**

Compute  $\mathcal{F}(X)$  based on

$$\text{QoS}_{\text{satisfied}} = \sum_{i=1}^{N_{\text{UE}}} \mathbb{1}(\text{SINR}_i \geq \text{SINR}_{\text{min}})$$

$$\text{SINR}_i = \frac{P_{\text{Tx}}}{\sum_{j \neq i} P_{\text{Int},j} + \eta}$$

**Step 3: Apply Mutation Operators**

**while** *Convergence criteria not met* **do**

**Step 3.1: In-Chromosome Mutators**

Apply:

Section Swapping: Swap segments within  $x_u \in X$ .

Point Insertion: Adjust task sequence to minimize cost:

$$\text{Cost}(x_u) = \sum_{i=1}^k (d_{i,u} + P_{\text{hover}} \cdot t_{\text{hover}}).$$

**Step 3.2: Cross-Chromosome Mutators**

Apply:

Task Swapping: Exchange tasks between  $x_u$  and  $x_v$ ,  $u \neq v$ .

Join Mutator: Merge paths for leader UAV coordination.

Separation Mutator: Split paths to balance task loads.

**Step 3.3: Update Paths**

Update paths  $X$  based on the mutation results.

$$X \leftarrow \{x'_1, x'_2, \dots, x'_{N_{\text{UAV}}}\}.$$

**Step 3.4: Re-Evaluate Fitness**

Recompute  $\mathcal{F}(X)$  by considering the updated paths, SINR constraints, and UAV capacity as follows:

$$\mathcal{F}(X) = \sum_{u=1}^{N_{\text{UAV}}} \left( \frac{1}{L(X_u)} + \frac{\text{QoS}_{\text{satisfied}}}{\text{QoS}_{\text{total}}} - \frac{E_{\text{cost}}(X_u)}{E_{\text{max}}} \right).$$

**end**

**Step 4: Output Results**

**return**  $X^* = \arg \max \mathcal{F}(X)$ .



This ensures that the algorithm continually favors configurations that enhance the performance metrics. The process terminates when convergence criteria are satisfied, such as achieving a stable fitness value or reaching the maximum number of iterations. The final solution  $X^*$  is selected as the chromosome with the highest fitness value

$$X^* = \arg \max \mathcal{F}(X) \quad (32)$$

This algorithm integrates advanced genetic operations to optimize the UAV task allocation and path planning. Balancing path efficiency and QoS compliance ensures robust and scalable solutions for dynamic UAV swarm operations. Its iterative nature and use of fitness-driven mutations make it adaptable to complex real-world scenarios. The use of SINR as a QoS metric and mutation operators tailored to UAV-specific constraints sets this algorithm apart from its application to UAV-based communication networks.

#### 4.2. Integration of the Proposed Advanced Fitness Function with QoS, Capacity Constraints, and Mutation for Optimization

Algorithm 3 defines a genetic optimization framework for UAV swarm path planning, ensuring that QoS metrics and UAV capacity constraints are considered. The algorithm begins with initializing the population ( $v_1$ ) from the initial paths ( $X_{init}$ ). In this step, UEs are assigned to UAVs based on their proximity and the task of each UAV  $u$  is represented as  $x_u = \text{UEs assigned to UAV } u, \forall u \in N_{UAV}$ . Additional variables, such as fitness, penalties, suma, and the service and angle ratios, were initialised to track the performance of each chromosome during the optimization process.

In the evaluation phase, the fitness of each chromosome  $X \in v_1$  is calculated using the fitness function

$$\mathcal{F}(X) = w_{SR} \cdot SR + w_{QoS} \cdot QoS_{satisfied} - w_{Penalty} \cdot \sum_{j \in Q} \max(0, Load_j - C_j) \quad (33)$$

where SR represents the service ratio,  $QoS_{satisfied}$  quantifies how well the QoS constraints are satisfied, and the penalty term ensures that UAVs that exceed their capacity  $C_j$  are penalized. The intersection ratio (IR) is computed as  $IR = \frac{\min(\Phi)}{\Phi_k}, \forall k \in \text{set}[\Phi]$ , which minimizes the number of trajectory conflicts by penalizing chromosomes with high-path intersections. The angle ratio (AR) is computed as  $AR = \frac{\sum \text{angle\_ratios}}{\text{len}(\mathcal{C})}$ , ensuring smoother UAV paths by penalizing the sharp angles. Together, these metrics update the fitness of each chromosome based on its path efficiency, service quality, and compliance with UAV capacity constraints.

The algorithm proceeds through the GA process and iterates until the convergence criteria are satisfied. In the selection phase, the roulette wheel method selects the parent chromosomes based on their fitness scores. The selection probability of each chromosome  $x$  is calculated as

$$\text{Selection Probability} = \frac{\mathcal{F}(x)}{\sum_{x' \in v} \mathcal{F}(x')} \quad (34)$$

to ensure that the fitter chromosomes are more likely to be selected. This mechanism promotes the survival of high-performance solutions for the next generation.

Following selection, the crossover is applied to the selected parents with probability  $p_c$ . The crossover operation combines the genes of the two parent chromosomes to generate offspring that inherit traits from both parents. The resulting child chromosome is represented by  $x_{child} = \text{Crossover}(x_{parent1}, x_{parent2})$ . This step enhances diversity within the population and facilitates the exploration of the solution space.

**Algorithm 3:** Advanced fitness function with QoS and capacity constraints

**Data:**  $V$ : Cluster centroids,  $\mathcal{C}$ : Chromosome set,  $\mathcal{U}$ : Unserviced set, Threshold  $\tau$ , UAV capacity  $C_{UAV}$ , QoS constraints,  $p_c$ : Crossover rate,  $p_m$ : Mutation rate.

**Result:** Optimized paths  $X^*$ .

**Initialize Variables:**

Initialise the population  $\nu_1$  from  $X_{init}$  by assigning UEs to UAVs based on proximity.

$$x_u = \text{UEs assigned to UAV } u, \quad \forall u \in N_{UAV}.$$

Initialise fitness, penalties, ratios,  $\text{suma}$ ,  $\text{service\_ratios}$ , and  $\text{angle\_ratios}$ ;

**Evaluate Initial Fitness:**

**foreach** chromosome  $X \in \nu_1$  **do**

  Compute the fitness:

$$\mathcal{F}(X) = w_{SR} \cdot SR + w_{QoS} \cdot QoS_{satisfied} - w_{Penalty} \cdot \sum_{j \in Q} \max(0, Load_j - C_j).$$

  Calculate Intersection Ratio (IR)

$$IR = \frac{\min(\Phi)}{\Phi_k}, \quad \forall k \in \text{set}[\Phi].$$

  Calculate Angle Ratio (AR) using

$$AR = \frac{\sum \text{angle\_ratios}}{\text{len}(\mathcal{C})}.$$

  Update the fitness based on path length, UAV capacity, and unserved UEs.

**end**

**Genetic Algorithm Process:**

**while** Convergence criteria not met **do**

**Selection:**

  Perform a roulette-wheel selection to choose parent chromosomes based on fitness.

$$\text{Selection Probability} = \frac{\mathcal{F}(x)}{\sum_{x' \in \nu} \mathcal{F}(x')}.$$

**Crossover:**

  Perform crossover with probability  $p_c$ :

$$x_{child} = \text{Crossover}(x_{parent1}, x_{parent2}).$$

**Mutation:**

  Apply mutation to the child chromosomes with probability  $p_m$

$$x' = \text{Mutate}(x_{child}, p_m),$$

**Evaluate Fitness:**

  Compute the updated fitness values  $\mathcal{F}(X)$  for the new chromosomes:

$$SINR_i = \frac{P_{Tx}}{\sum_{j \neq i} P_{Int,j} + \eta}, \quad SINR_i \geq SINR_{min}.$$

**Update Population:**

  Replacing the least-fit chromosomes in a population with new offspring.

**end**

**Output Optimized Paths:**

Return:

$$X^* = \arg \max \mathcal{F}(X).$$

Next, mutation is applied to the child chromosomes with probability  $p_m$ . Mutation introduces random changes to the genes of a chromosome, thereby ensuring that new areas in the solution space are explored. The mutated chromosome is represented by  $x' = \text{Mutate}(x_{\text{child}}, p_m)$ . This step helps prevent premature convergence by maintaining the genetic diversity in the population [29].

After performing crossover and mutation, the fitness values of the updated population were re-evaluated. This step includes computing the SINR for each chromosome to ensure that QoS constraints are satisfied. The SINR for a given UAV  $i$  is calculated as

$$\text{SINR}_i = \frac{P_{\text{Tx}}}{\sum_{j \neq i} P_{\text{Int},j} + \eta} \quad (35)$$

where  $P_{\text{Tx}}$  is the transmitted power,  $P_{\text{Int},j}$  represents the interference from neighboring UAVs, and  $\eta$  is the noise power. The algorithm ensures that  $\text{SINR}_i \geq \text{SINR}_{\text{min}}$  penalizes chromosomes that fail to satisfy this requirement.

Finally, the population is updated by replacing the least-fit chromosomes with newly generated offspring. The algorithm terminates when the convergence criteria are satisfied, such as reaching the maximum number of iterations or achieving a stable fitness value across generations. The optimal solution  $X^*$  is then selected as the chromosome with the highest fitness value, expressed as

$$X^* = \arg \max \mathcal{F}(X) \quad (36)$$

This algorithm efficiently balances the service quality, path optimization, and capacity constraints, making it suitable for dynamic UAV swarm operations in complex environments. Incorporating multiple fitness metrics and leveraging genetic operations provides a robust framework for UAV path planning and task allocation.

$$\begin{aligned} \text{Score} = & w_{\text{SR}} \cdot \text{SR}^2 + w_{\text{AR}} \cdot \text{AR} + w_{\text{DR}} \cdot \log(\text{DR}) \\ & + w_{\text{IR}} \cdot \text{IR} + w_{\text{PSR}} \cdot \text{PSR} - w_{\text{Penalty}} \cdot \sum_{j \in Q} \max(0, \text{Load}_j - C_j) \\ & + w_{\text{QoS}} \cdot \text{QoS}_{\text{satisfied}} \end{aligned} \quad (37)$$

Equation (37) presents a multi-factor fitness scoring mechanism designed to optimize UAV swarm configurations for disaster response networks. It integrates various performance metrics into a single score to ensure comprehensive evaluation and optimization. The term  $w_{\text{SR}} \cdot \text{SR}^2$  emphasizes the service coverage and prioritizes configurations with extensive coverage by amplifying the service ratio (SR) through squaring. This ensures that candidates with better connectivity have a higher chance of selection. The angular ratio (AR), represented by  $w_{\text{AR}} \cdot \text{AR}$ , promotes smoother UAV paths, minimizing abrupt changes that can disrupt communication. The logarithmic term  $w_{\text{DR}} \cdot \log(\text{DR})$  ensures that the data rate contributions are impactful but balanced, reflecting the diminishing returns of the increasing throughput. Similarly, the  $w_{\text{IR}} \cdot \text{IR}$  term penalizes the interference, favoring configurations with reduced co-channel interference for better signal quality. Path smoothness, captured by  $w_{\text{PSR}} \cdot \text{PSR}$ , ensures efficient UAV trajectories and reduces operational complexity. A dynamic penalty mechanism,  $w_{\text{Penalty}} \cdot \sum_{j \in Q} \max(0, \text{Load}_j - C_j)$ , discourages base station overloading, maintains scalability, and avoids congestion. The QoS term  $w_{\text{QoS}} \cdot \text{QoS}_{\text{satisfied}}$  rewards a configuration that meets user satisfaction thresholds, reflecting the system's adaptability to varying network conditions. Weights ( $w_{\text{SR}}, w_{\text{AR}}, w_{\text{DR}}, w_{\text{IR}}, w_{\text{PSR}}, w_{\text{Penalty}}, w_{\text{QoS}}$ ) balance the importance of each metric, allowing the equation to adapt to specific scenarios such as high-demand or interference-prone areas. This equation is based on prior methodologies [29,37] that incorporate advancements in trajectory optimization, QoS prioritization,

and resource allocation. It ensures scalable and resilient UAV deployment by dynamically adapting to environmental conditions and user needs. Furthermore, the computational efficiency is enhanced by iterative updates to the unserved UE dataset and fixed-interval calculations, balancing the accuracy and processing overhead. Overall, Equation (37) encapsulates a robust, adaptable scoring framework that addresses the multifaceted requirements of disaster response networks, significantly outperforming traditional approaches.

As shown in Figure 4, the distribution of UEs across different environments (suburban, urban, dense urban, and high-rise urban) highlights the initial setup and service allocation before and after the implementation of the swarm UAV solution. The subplots represent the total number of UEs, serviced, and unserved under varying user densities ranging from 50 to 450.

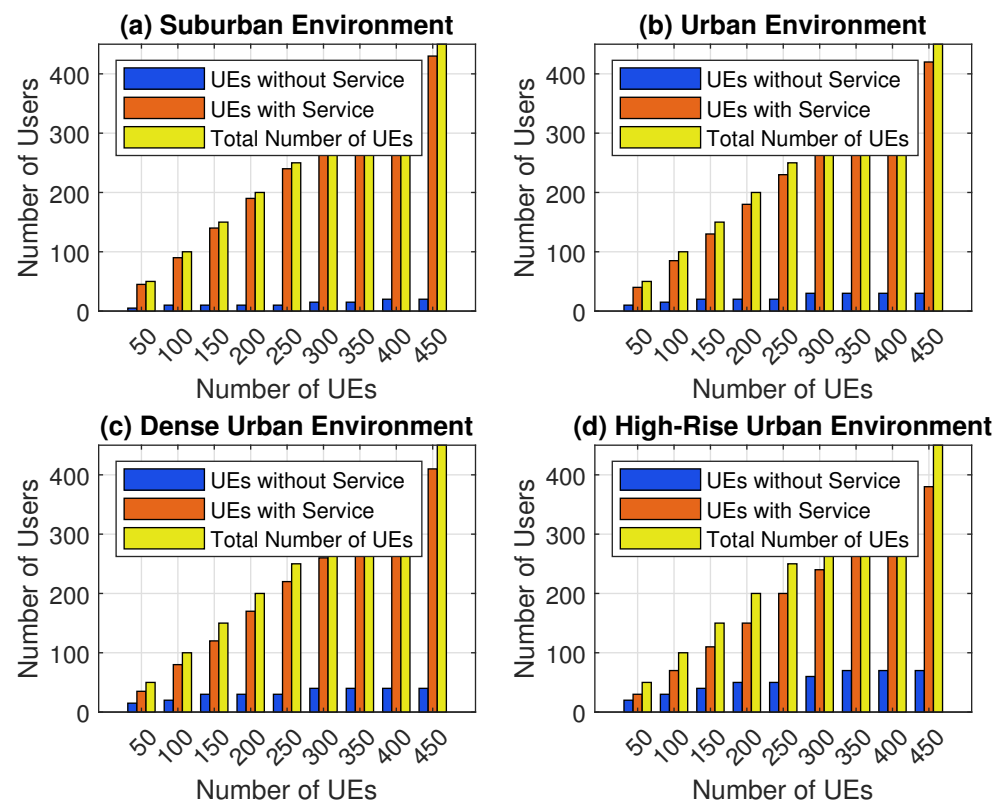


**Figure 4.** Initial Setup of UEs in different environments.

The comparison between serviced and unserved UEs reflects the adaptive capabilities of the swarm UAV solution. For example, the **suburban** environment exhibits the highest percentage of UEs with services across all user densities, achieving 95% service rates when the UE count reaches 450. This is primarily attributed to better LOS conditions and reduced interference, which improve the signal propagation and connectivity. In contrast, the **high-rise urban** environment has the lowest service rate, with only 85% of UEs receiving services at maximum user density. This is owing to increased signal attenuation, multipath interference, and the challenges posed by NLOS propagation in high-rise settings.

The **urban** environment serves as a middle ground between the suburban and dense urban scenarios. While achieving slightly lower service rates than suburban areas, the urban environment demonstrates a relatively consistent performance across increasing user densities, with service rates stabilizing at approximately 90% at high user densities. The combination of a moderate building density and manageable interference levels in this environment facilitates this balance.

The **dense urban** and high-rise urban environments, however, show a gradual increase in unserved UEs as user density increases. This reflects the impact of spatial constraints and interference, which limit the effective range of the UAV-based base stations. In contrast, the suburban environment demonstrates the adaptive capabilities of the swarm UAV solution, where the number of unserved UEs remains consistently low, even as the user density increases.

The significance of this initial UE organization lies in its ability to identify coverage gaps and optimize swarm UAVs deployment strategies. By clustering UEs in areas with high service demand, swarm UAVs can allocate resources more efficiently, ensuring that critical regions are prioritized. This process directly addresses fundamental wireless communication challenges such as load balancing, interference management, and signal optimization.

Furthermore, the observed variations in service levels across environments emphasize the need for environment-specific optimization strategies. For example, high-rise urban settings may benefit from higher-density UAV swarms or hybrid deployment models that combine static and mobile base stations to mitigate coverage loss. Similarly, in suburban areas, favorable propagation conditions present opportunities for maximizing energy efficiency while maintaining high service quality.

In summary, the distribution of UEs and their service status underscores the importance of adaptive clustering algorithms and environment-specific strategies in disaster response networks. The ability of swarm UAVs to dynamically adjust their deployment based on user density and environmental constraints ensures a robust and scalable solution for improving coverage, connectivity, and QoS across diverse scenarios. This foundational analysis forms the basis for further optimization efforts, particularly in environments with complex topographical and network challenges.

## 5. Performance Evaluation of Proposed Solution

### 5.1. Evaluation Criteria and Experimental Setup

The evaluation criteria for the proposed MABS solution were systematically chosen to comprehensively assess the path planning efficiency and overall performance in diverse disaster response scenarios. Key parameters include the coverage ratio, QoS compliance, and fitness scores. These metrics provide insights into the effectiveness of the solution for managing network coverage, resource allocation, and user QoS under dynamic conditions. In addition, the impact of mobility models on network performance, as well as the scalability of the solution with increasing swarm UAVs, was analyzed to validate its robustness and reliability.

The evaluation includes comparisons between the proposed method (GA + APC) and established benchmarks, such as GA, PSO, and ACO. These comparisons not only highlight the relative strengths of the solutions but also emphasize their practical utility in disaster response networks. Each metric was carefully analyzed to demonstrate tangible improvements in performance, scalability, and operational efficiency, particularly under challenging conditions typical of disaster environments.

To validate the proposed MABS solution, a series of simulations were conducted involving UAV swarms (1 to 10) and UE ranging from 50 to 450. These scenarios were modeled across four distinct environments: suburban, urban, dense urban, and high-rise urban, with varying propagation characteristics such as LOS and NLOS conditions. The placement of the UE and base stations was randomized, following a Poisson distribution with a spatial density of  $25 \text{ km}^2$ .

Simulations were designed to measure metrics such as coverage ratio, QoS compliance, and fitness score over iterations ranging from 1 to 17,000, as shown in Table 2. The mobility

impact was assessed by comparing the RWPM and RPGM models. By iteratively optimizing the UAV swarm deployment and path planning, the experiments aimed to determine the optimal configurations for maximizing coverage and service quality, while minimizing resource consumption.

Table 3 outlines the local simulation parameters and configurations used to evaluate the performance of the UAV swarm in the studied disaster response environment. The table provides detailed specifications of the environment parameters. These parameters serve as the foundation for assessing the scalability, adaptability, and reliability of networks under various operational conditions. The environment is categorized into four distinct scenarios: urban ( $E_1$ ), suburban ( $E_2$ ), dense urban ( $E_3$ ), and high-rise urban ( $E_4$ ), each characterized by specific path-loss parameters ( $a$ ,  $b$ ), LOS, and NLOS attenuation factors. These scenarios represent diverse terrain complexities encountered in real-world operations. The path-loss parameters and attenuation factors are based on well-established communication models and reflect the propagation characteristics unique to each environment [39]. None of the other works discussed in Section 2 perfectly fit within the framework that was considered in this study, and thus, for fairness of comparison, were not included. The closest work to this effort is [29,37]; however, because this work introduces swarm-UAVs, different QoS requirements, mobility models, and dynamic environments to this framework, it makes a direct comparison with these works difficult, except if they are used as a special case. For this reason, this work focuses on comparing the proposed hybrid APC-GA algorithm with other algorithms such as GA, PSO, and ACO in different environments and studying metrics such as coverage and latency. Furthermore, the latency metric was introduced into the framework in dynamic disaster scenarios and adaptive mobility modeling for the first time.

**Table 3.** Local simulation parameters and settings for UAV swarms [29,30,37,38].

Category	Parameter	Notation/Value	Description
Environment Parameters	$E_1$ (Urban)	$a = 9.61, b = 0.43, \eta_{\text{LOS}} = 0.1,$ $\eta_{\text{NLOS}} = 20$	Path loss parameters for urban environments.
	$E_2$ (Suburban)	$a = 4.88, b = 0.43, \eta_{\text{LOS}} = 0.1,$ $\eta_{\text{NLOS}} = 21$	Suburb-specific signal-propagation characteristics.
	$E_3$ (Dense Urban)	$a = 12.08, b = 0.11, \eta_{\text{LOS}} = 1.6,$ $\eta_{\text{NLOS}} = 23$	Parameters for densely populated urban environments.
	$E_4$ (High-Rise Urban)	$a = 27.23, b = 0.08, \eta_{\text{LOS}} = 2.3,$ $\eta_{\text{NLOS}} = 34$	Parameters of high-rise urban areas.

## 5.2. Coverage Ratio vs. Number of UAV Swarms

### 5.2.1. Dense Urban Environment

In Figure 5, dense urban environments, the presence of tall buildings, and complex layouts often introduce severe challenges to wireless communication, such as signal blockages and increased interference. The results highlight the capability of the proposed GA + APC method to handle such conditions effectively. With a coverage ratio peaking at 97% when 10 UAV swarms are deployed, the method demonstrates its adaptability and strength in optimizing coverage despite high-density obstacles.

Interestingly, although the GA, PSO, and ACO benchmarks also showed improvements as the number of UAV swarms increased, their growth was noticeably slower. For example, the GA only reaches 91% coverage, suggesting that traditional optimization approaches lack the nuanced adaptability of the proposed method. The collaborative nature of GA + APC, which leverages both genetic evolution and path control, plays a crucial role in achieving superior performance.

This environment highlights the critical importance of dynamic path planning, particularly in limited LOS communication scenarios. By strategically navigating these challenges, the proposed method is a reliable choice for dense urban deployment.

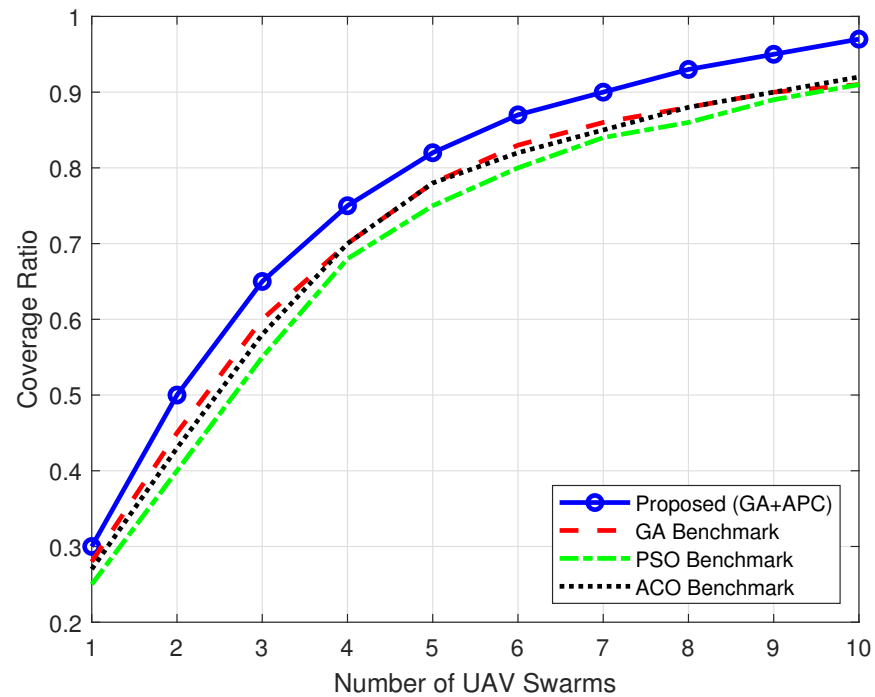


**Figure 5.** Coverage ratio vs. number of UAV swarms in dense urban environment.

### 5.2.2. Urban Environment

In Figure 6, the urban environments represent a middle ground between dense urban and suburban conditions with moderately distributed obstacles and user densities. The proposed GA + APC method achieved a coverage ratio of 94% with 10 UAV swarms, which surpassed all benchmarks, including GA (89%), PSO (88%), and ACO (89%).

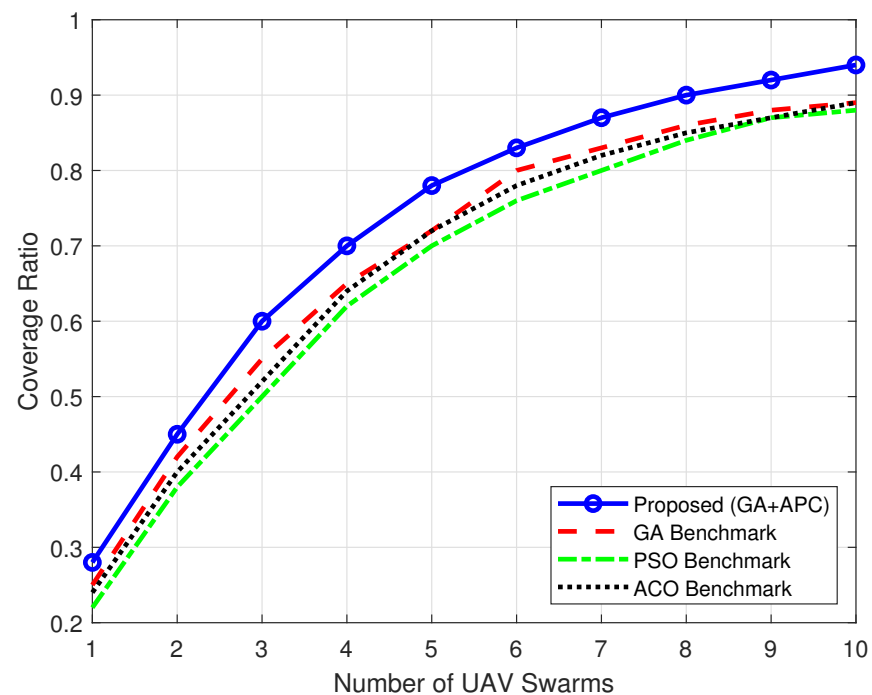


**Figure 6.** Coverage ratio vs. number of UAV swarms in urban environment.

The relatively smaller performance gap among the methods compared to dense urban scenarios suggests that less complex propagation conditions allow all algorithms to perform reasonably well. However, the consistent outperformance of GA + APC highlights its ability to extract additional efficiency by allocating swarm UAV resources. Notably, the diminishing returns in coverage improvement beyond eight UAV swarms reveal a natural coverage saturation point, where additional swarm UAVs contribute minimally to the overall system performance.

### 5.2.3. Suburban Environment

Figure 7 highlights that suburban environments, characterized by open spaces and minimal interference, exhibit the highest overall coverage ratios among all scenarios. The results show that the proposed GA + APC method achieved 100% coverage with only nine UAV swarms. This is a remarkable feature, especially when compared with GA (99%), PSO (98%), and ACO (98%).

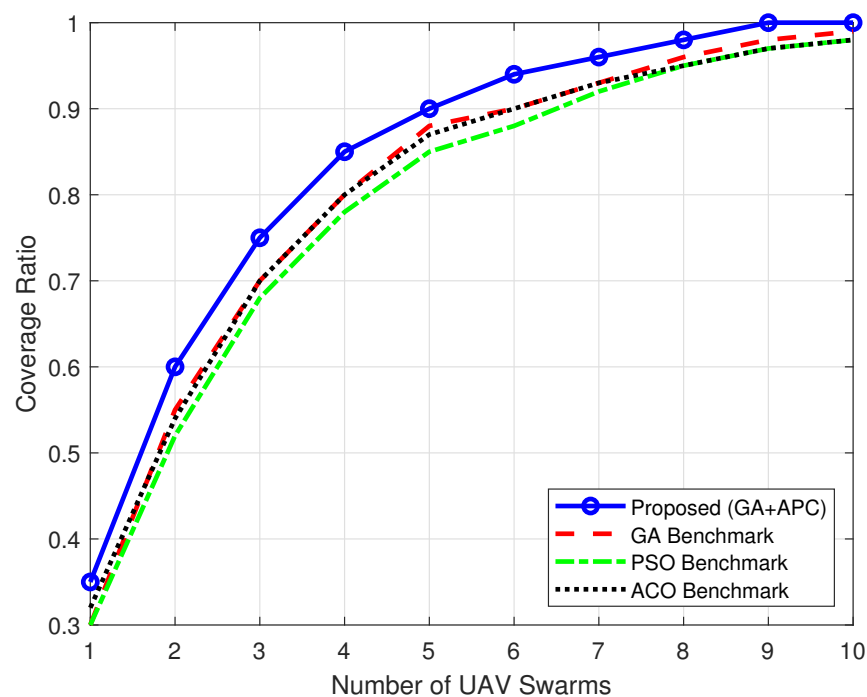


**Figure 7.** Coverage ratio vs. number of UAV swarms in suburban environment.

These findings underscore the efficiency of the proposed method in leveraging favorable propagation conditions to minimize resource usage while maximizing coverage. The benchmarks, while performing admirably, failed to match the resource efficiency of GA + APC, indicating a lack of fine-grained adaptability to dynamic user distributions. This scenario reinforces the value of advanced optimization techniques in ensuring effective swarm UAV deployment, particularly in resource-limited situations.

### 5.2.4. High-Rise Urban Environment

The results for high-rise urban environments are shown in Figure 8 and present a unique set of challenges owing to the vertical nature of obstacles and severe NLOS propagation effects. In this setting, the proposed GA + APC method achieved a coverage ratio of 93% with 10 UAV swarms, outperforming the GA (88%), PSO (85%), and ACO (88%).

What stands out is the ability of the method to adapt to highly variable and unpredictable signal conditions. The benchmarks exhibit slower coverage improvement, with PSO showing particularly limited performance owing to its inherent reliance on simpler



optimization strategies. The proposed method, on the other hand, benefits from its continuous adaptability, enabling it to navigate the constraints of vertical environments effectively. This capability is crucial for ensuring reliable communication in high-rise urban settings where maintaining consistent coverage is often challenging.

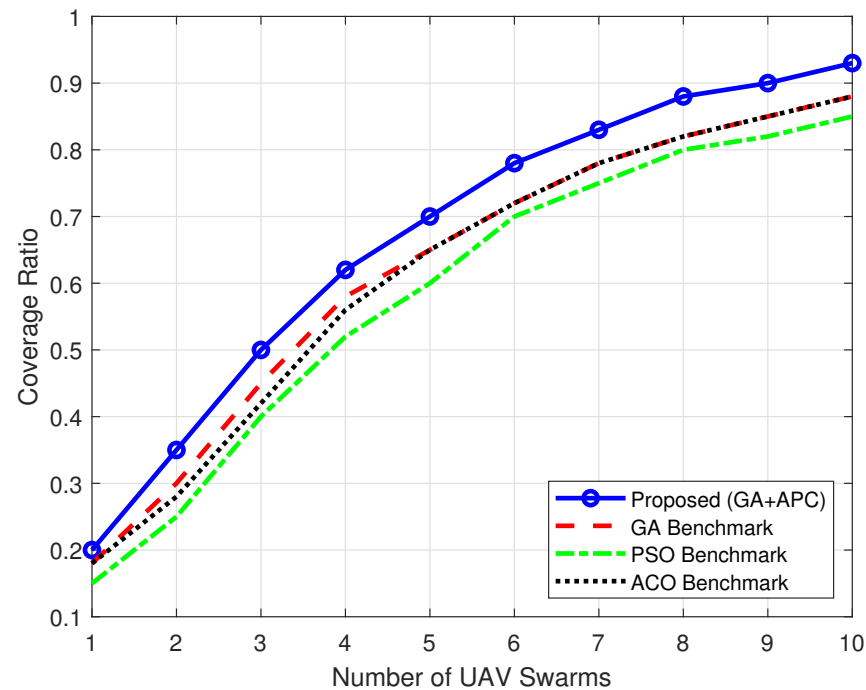


**Figure 8.** Coverage ratio vs. number of UAV swarms in high-rise urban environment.

Across all environments, the results reveal a clear pattern: the proposed GA + APC method consistently outperforms traditional benchmarks, with its advantage being most pronounced in challenging scenarios such as dense urban and high-rise urban areas. This performance can be attributed to its adaptive path planning, intelligent resource allocation, and its ability to handle complex interference patterns. The findings also emphasize the importance of tailoring swarm UAV deployment strategies according to the specific characteristics of each environment. While suburban areas benefit from minimal swarm UAV usage owing to favorable conditions, urban and dense urban environments require more sophisticated optimization to address interference and NLOS challenges. The scalability and robustness of the proposed method make it a versatile choice for diverse disaster response scenarios. In summary, these results highlight the growing importance of collaborative and adaptive optimization approaches in swarm UAV-based communication. By dynamically adjusting to environmental challenges, the proposed GA + APC method offers a compelling solution for enhancing the coverage and reliability of critical disaster response networks.

The deployment of swarm UAVs has demonstrated remarkable success in restoring the communication infrastructure in disaster-stricken areas, as depicted in Figures 5–8. The proposed method (GA + APC) consistently outperformed traditional benchmarks, achieving higher coverage ratios with fewer UAVs. In suburban environments, the solution achieved nearly 100% coverage with 10 UAV swarms, whereas urban and dense urban settings achieved coverage ratios of 94% and 97%, respectively. This superior performance is attributable to the adaptive clustering mechanism that optimizes UAV placement and path planning. Figures 5–8 further illustrate the relationship between the number of UAV swarms and coverage in dense urban, urban, suburban, and high-rise urban environments, respectively. Despite the challenging propagation conditions, the proposed method achieved 93% coverage with 10 UAVs, significantly outperforming the ACO benchmark,

which achieved only 88% coverage under similar conditions. These results emphasize the ability of the solution to address NLOS challenges and interference, which are common in urban disaster scenarios.

The path planning optimization enabled by GA + APC is a key factor in achieving high coverage ratios. As shown in Figures 5–8, the coverage ratios across all environments increase significantly with the number of UAV swarms, demonstrating the scalability of the solution. The suburban environment, with its open topology and minimal interference, experienced the fastest improvement in coverage, reaching 100% with only eight UAV swarms. In contrast, dense urban and high-rise environments require up to 10 UAVs to achieve maximum coverage owing to increased propagation challenges.

The results in Table 4 demonstrate the performance of the proposed GA + APC method in various operational environments, illustrating its adaptability and robustness for addressing distinct communication challenges. In dense urban areas, where obstacles such as tall buildings and severe interference impede communication, GA + APC achieved a coverage ratio of 97%, significantly outperforming traditional benchmarks such as GA, which attained a maximum of 91%. This outcome underscores the efficacy of GA + APC's dynamic path planning and optimization capabilities in surmounting NLOS challenges and interference.

**Table 4.** Comparative table summarizing the findings.

Environment	GA + APC Coverage Ratio	Best Benchmark Coverage Ratio	Key Observations
Dense Urban Environment	97%	91% (GA)	GA + APC excels in managing severe interference and NLOS conditions through adaptive path planning, achieving significant improvement over traditional methods.
Urban Environment	94%	89% (GA,ACO)	Moderate performance gap owing to less complex propagation conditions; GA + APC maintains consistent superiority and resource efficiency.
Suburban Environment	100%	99% (GA)	Favorable conditions allow all methods to perform well, but GA + APC achieves complete coverage with fewer UAVs, emphasizing resource efficiency.
High-Rise Urban Environment	93%	88% (GA,ACO)	GA + APC effectively navigate vertical obstacles and severe NLOS challenges, demonstrating strong adaptability in complex environments.

In urban environments, the proposed method maintained its advantage, achieving 94% coverage compared with 89% achieved by GA and ACO. The reduced performance differential reflects the relatively less complex propagation conditions in these scenarios. Nevertheless, GA + APC's consistently superior performance underscores its capacity to optimize resource allocation and adapt to dynamic user distributions, ensuring efficient coverage even in moderately challenging environments.

In suburban areas, which are characterized by open spaces and minimal interference, the proposed method achieved full coverage (100%) with only nine UAV swarms. This demonstrates its capacity for resource-efficient operation, particularly in scenarios with favorable communication conditions. Although traditional benchmarks such as GA (99%) and PSO (98%) performed well, they did not attain the same level of efficiency.

The results in high-rise urban environments further substantiate the advantages of GA + APC, demonstrating a coverage ratio of 93% compared with 88% for GA and ACO.

The vertical nature of obstacles in this scenario presents significant propagation challenges. However, the proposed method consistently adapts to unpredictable signal conditions and ensures a reliable coverage.

These findings underscore the scalability and robustness of the GA + APC method under diverse deployment scenarios. Its capacity to optimize resource allocation and address complex interference patterns renders it a versatile solution for enhancing UAV swarm-based communication. This study further emphasizes the significance of tailoring deployment strategies to environmental characteristics. Dense and high-rise urban areas require advanced optimization to address interference and NLOS issues, while suburban areas permit minimal resource utilization owing to favorable conditions. Overall, the GA + APC method exhibits significant potential for improving communication reliability and efficiency in critical disaster response scenarios.

### 5.3. Fitness Score vs. Iterations

The fitness score results in Figure 9 reveal that the proposed method maintains significantly higher and more stable scores over 17,000 iterations compared with the benchmarks. Starting at 0.95, the fitness score of the proposed method decreased gradually, whereas benchmarks such as GA, PSO, and ACO exhibited lower starting values (0.9, 0.85, and 0.8, respectively) and greater variability. This represents an initial improvement of approximately 5.6% over GA, 11.8% over PSO, and 18.8% over ACO, respectively. Such improvements demonstrate the superior adaptability and stability of the proposed scheme under various conditions.

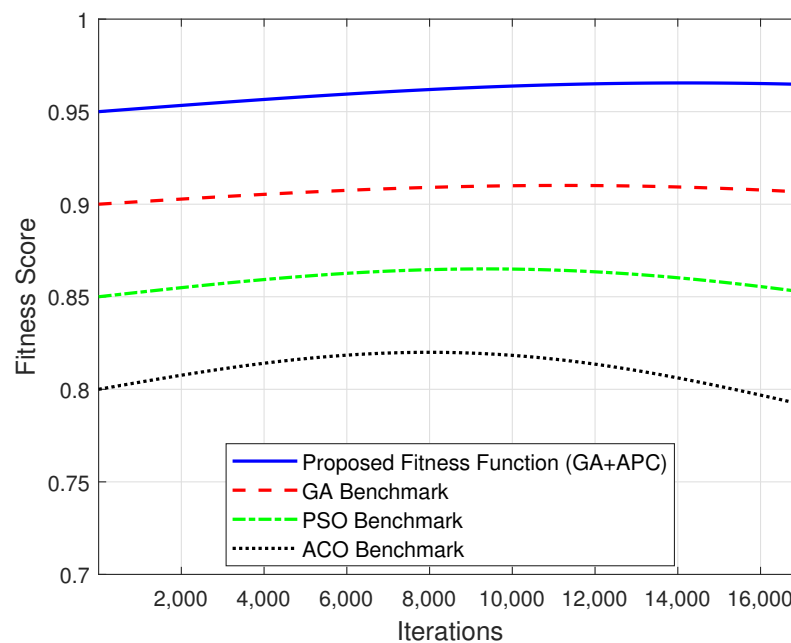


**Figure 9.** Fitness score vs. iterations for proposed function and benchmarks.

These results underscore the efficiency of the proposed method in maintaining optimal performance despite network dynamics, such as mobility and different QoS requirements. The slight decline in the fitness scores reflects the natural impact of mobility-induced topology changes and energy depletion. This behavior is consistent with real-world wireless communication networks, where dynamic user mobility necessitates periodic re-optimization to maintain performance. The variability of benchmarks highlights their susceptibility to suboptimal solutions, further emphasizing the robustness of the proposed fitness function in ensuring consistent path planning and resource allocation.

#### 5.4. QoS Compliance vs. Number of UAV Swarms

The proposed method in Figure 10 achieves the highest QoS compliance across all swarm configurations, with 98% compliance observed with 10 UAV swarms, compared to 94% for GA, 90% for PSO, and 92% for ACO. At lower swarm numbers (one UAV swarm), the proposed method achieves 85% compliance, surpassing the benchmarks of 80% for GA, 75% for PSO, and 78% for ACO. These results represent an improvement of 6.25% over GA, 13.33% over PSO, and 8.97% over ACO for lower swarm configurations. At higher swarm configurations (10 UAV swarms), the proposed method achieved an improvement of 4.26% over GA, 8.89% over PSO, and 6.52% over ACO. This demonstrated the scalability and superior performance of the proposed scheme across diverse swarm configurations.

The strong QoS compliance achieved by the proposed method reflects its ability to satisfy the stringent user requirements for data rates. This was achieved through efficient resource allocation and dynamic swarm UAVs positioning. The results also highlight the role of spatial diversity in enhancing network performance because increasing the number of swarm UAVs reduces resource contention and ensures more consistent service delivery. The lower compliance rates of the benchmarks can be attributed to their less effective optimization algorithms, which struggle to effectively allocate resources in high-demand scenarios.

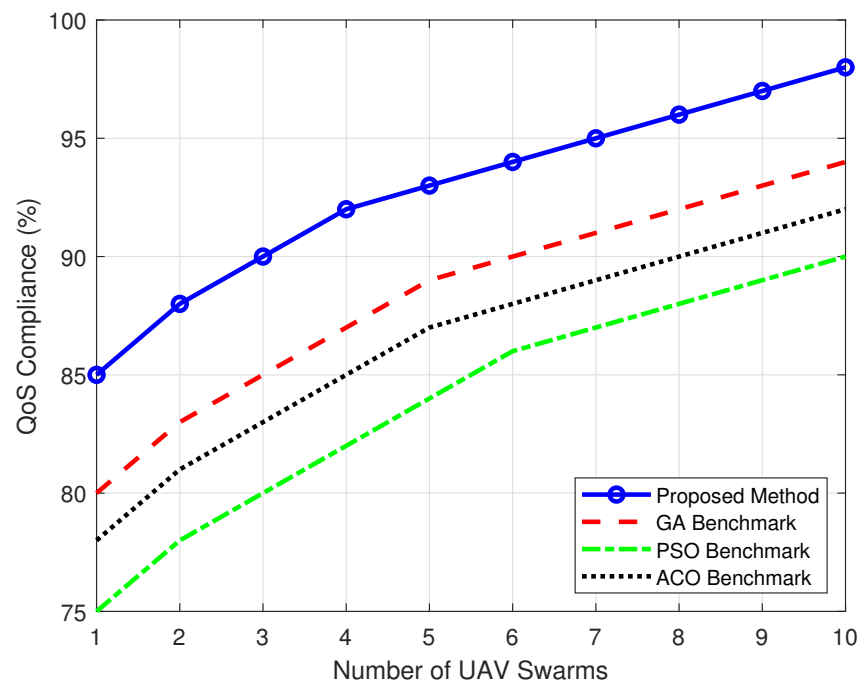
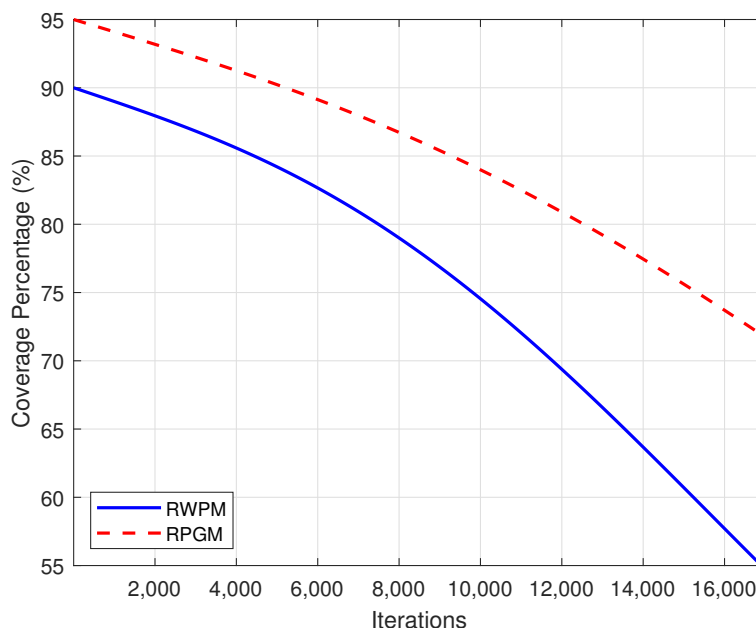


Figure 10. QoS compliance vs. number of UAV swarms.

#### 5.5. Mobility Impact on Coverage

As shown in Figure 11, the RPGM mobility model outperforms the RWPM model in terms of maintaining coverage over 17,000 iterations. While both models show a slight decline in coverage percentages over time, the RPGM model consistently achieves higher coverage due to its group mobility pattern. This result highlights the significant impact of mobility models on wireless communication performance. The ability of the RPGM to serve user clusters efficiently reduces the need for frequent swarm UAV repositioning, conserving energy, and enhancing coverage. This aligns with real-world disaster response scenarios, in which users often move in groups. The lower performance of the RWPM model indicates its inability to adapt to such mobility patterns, resulting in reduced coverage efficiency.

These findings underscore the importance of selecting appropriate mobility models to optimize network performance in dynamic environments.



**Figure 11.** Impact of mobility models on coverage provided by swarm UAVs.

The ability of the proposed method to dynamically adapt to environmental conditions is shown in Figure 9, which compares the fitness scores of the proposed solution with those of traditional benchmarks over 17,000 iterations. The stability of the fitness score, averaging 0.95, highlights the robustness of the method and its ability to consistently optimize UAV trajectories. This is particularly important in dynamic disaster scenarios, in which environmental conditions can change rapidly.

The QoS compliance of a solution is another area of significant improvement. Figure 10 shows that the proposed method achieved a compliance rate of 98% with 10 UAV swarms, compared to 94% for the GA benchmark and 90% for the PSO benchmark. This improvement is a direct result of the adaptive clustering and path planning mechanisms of the solution, which ensures that UAVs are strategically positioned to minimize latency and maximize throughput.

The analysis of the UE coverage across different environments, as shown in Figure 7, further elucidates the effectiveness of the solution. In suburban settings, 95–100% of UEs received services, even at higher user densities. Urban and dense urban environments, although more challenging, still achieved service rates exceeding 90%, highlighting the robustness of the solution in maintaining connectivity despite interference and high user density.

Figure 11 compares the coverage achieved under the two mobility models: RPGM and RWPM. RPGM consistently provided higher coverage, maintaining an average of 95% over 17,000 iterations compared with 90% for RWPM. This performance disparity can be attributed to the ability of the RPGM to simulate clustered user movements, which aligns better with the UAV swarm clustering algorithm. Conversely, the dispersed mobility pattern of RWPM posed greater challenges for coverage, emphasizing the need for tailored deployment strategies based on user mobility patterns.

### 5.6. Latency vs. Number of UAV Swarms

The formula used to compute latency across all environments is as follows:

$$L = L_0 + \frac{\alpha}{\text{Coverage Ratio}} - \beta \cdot N_{\text{UAV}} \quad (38)$$

$L_0$  (base latency) represents the fixed latency due to inherent system delays, such as processing time at the UAV, communication setup time, or other constant factors unrelated to coverage or swarm size. This was assumed to be constant across environments. In the term  $\frac{\alpha}{\text{Coverage Ratio}}$ , coverage ratio represents the proportion of users effectively covered by the UAV swarm. A higher coverage ratio generally reduces network delays because more users are served effectively.  $\alpha$  is a weight that controls the influence of the coverage ratio on latency. Larger values of  $\alpha$  indicate that insufficient coverage has a more significant impact on latency. The term  $\frac{\alpha}{\text{Coverage Ratio}}$  models the inverse relationship between coverage and latency: when coverage is low, fewer users are served and the network experiences congestion, leading to higher latency. The term  $-\beta \cdot N_{\text{UAV}}$  accounts for the fact that increasing the number of UAVs can reduce the load on individual UAVs and improve overall communication efficiency.  $N_{\text{UAV}}$  is the number of UAVs in the swarm. A larger swarm size allows for a better resource distribution, leading to reduced latency.  $\beta$  is a weight that quantifies how much latency is reduced per additional UAV in the swarm. Larger values of  $\beta$  indicate that adding more UAVs has a stronger effect on lowering latency.

#### 5.6.1. Dense Urban Environment

Figure 12 illustrates the outcomes for high-rise urban settings, which are characterized by intense interference, greater user concentration, and significant NLOS challenges. Due to the intricacy of the terrain and user distribution, all algorithms experience higher latency compared to suburban and urban environments. The GA + APC approach demonstrated the most rapid decrease in latency as the swarm size grew, capitalizing on its adaptive clustering and optimization abilities. Comparative methods like PSO and ACO exhibit slower latency reductions, indicating their limited capacity to dynamically adjust to severe NLOS conditions and high-density user distributions. While GA performs marginally better than PSO and ACO, it still falls short of the proposed method due to its inability to effectively consider real-time mobility and communication constraints. The GA + APC method exhibited superior adaptability and resource efficiency in densely populated urban areas, making it particularly well-suited for environments with high interference and user density.

#### 5.6.2. Urban Environment

Figure 13 displays the outcomes for urban settings. These environments present greater challenges due to higher user concentrations and elevated interference levels. Despite this, the GA + APC approach consistently achieves lower latency than other methods across all swarm sizes, with a more pronounced decrease in latency as UAV swarm numbers grow. While techniques like GA and PSO show moderate performance, they struggle to match the GA + APC method's adaptability, especially in scenarios with fewer UAV swarms. ACO demonstrates the highest latency, attributed to its slower convergence and less flexible path planning capabilities in this context. The GA + APC approach effectively manages the heightened user density and interference typical of urban environments, showcasing its resilience under moderately complex conditions.

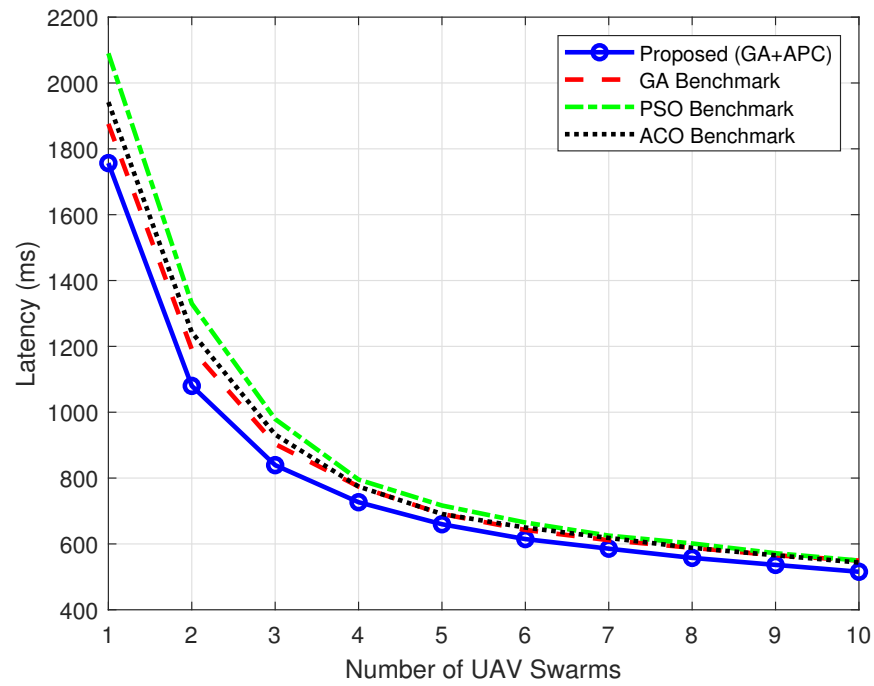


Figure 12. Latency vs. number of UAV swarms in dense urban environment.

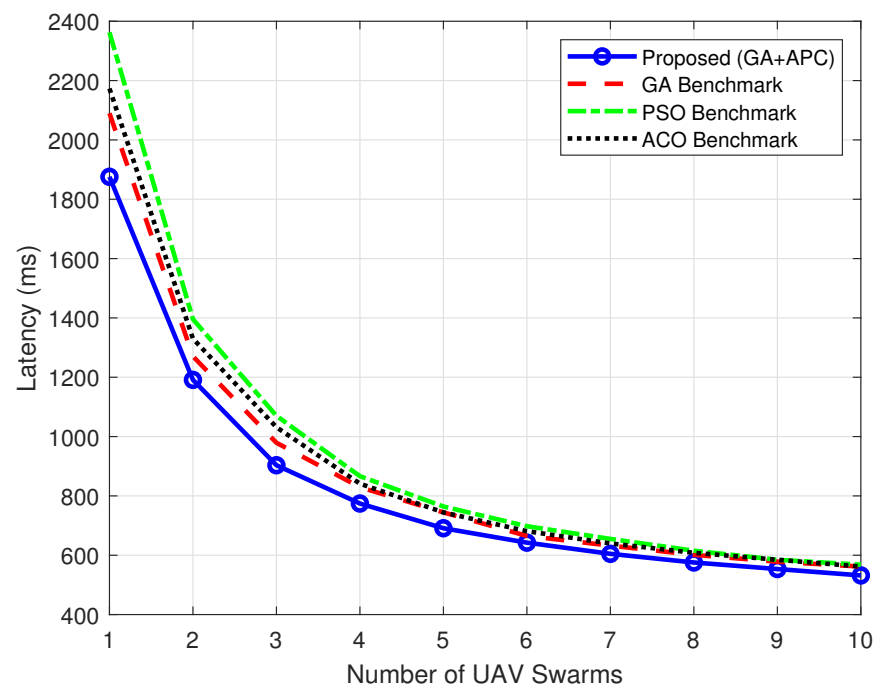
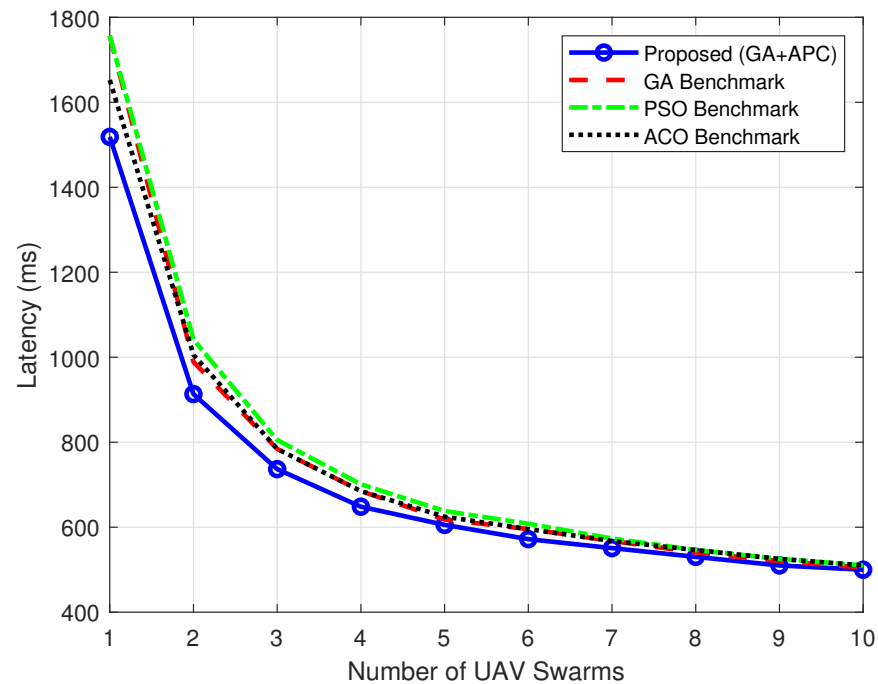


Figure 13. Latency vs. number of UAV swarms in urban environment.

### 5.6.3. Suburban Environment

Figure 14 displays the outcomes for suburban settings, where all algorithms exhibit consistently low latency due to favorable conditions, including fewer obstacles and a relatively uniform user distribution. As the number of UAV swarms grows, the proposed GA + APC technique surpasses the benchmark methods (GA, PSO, and ACO). At lower swarm counts, higher latency is observed due to limited coverage and increased user-to-UAV ratios. Nevertheless, the GA + APC approach minimizes latency by dynamically optimizing UAV trajectories and clusters based on user mobility and communication requirements. Latency decreases markedly as swarm size increases, indicating improved coverage and more efficient resource allocation. The benchmark algorithms (GA, PSO, and

ACO) demonstrate slower latency reductions, underscoring the limitations of their static or less adaptive optimization strategies in addressing dynamic user needs. The suburban environment showcased the scalability of the proposed method, achieving near-optimal latency with larger swarm sizes.



**Figure 14.** Latency vs. number of UAV swarms in suburban environment.

#### 5.6.4. High-Rise Urban Environment

Figure 15 illustrates the outcomes for high-rise urban settings, which present the most significant challenges due to vertical obstructions, extreme NLOS conditions, and irregular user distribution. These factors contribute to the highest latency across all algorithms compared to other environments, highlighting the complexity of maintaining uninterrupted communication in such intricate scenarios. The GA + APC approach surpassed the benchmark methods, demonstrating notably reduced latency as swarm sizes increased. Its capacity to dynamically adjust UAV trajectories around obstacles and enhance communication pathways ensures superior performance. Benchmark algorithms like PSO and ACO show minimal improvement in latency reduction with larger swarm sizes, indicating their limited efficacy in navigating vertical barriers and sustaining QoS compliance. While the GA exhibits moderate enhancements, it falls short of matching the adaptability and efficiency of the proposed GA + APC method. This approach excels in high-rise urban environments by effectively addressing vertical obstacles and severe NLOS challenges, thereby maintaining low latency.

The GA + APC approach consistently demonstrated the lowest latency in all environments, showcasing its adaptability and effectiveness in managing dynamic user distributions and communication needs. Suburban and urban settings exhibited comparatively low latency due to fewer obstructions and moderate user density. More challenging conditions were presented by dense urban Figure 12 and high-rise urban Figure 15 environments, where latency remained higher because of complex terrains and severe NLOS conditions. The proposed method's adaptability ensured superior performance in these demanding scenarios. The benchmark algorithms (GA, PSO, and ACO) showed varying degrees of effectiveness. GA performed relatively well in urban and dense urban environments, while PSO and ACO struggled in more complex settings. The GA + APC method consistently



outperformed all benchmarks, especially in high-density and high-obstacle environments, underscoring its robustness and efficiency. These results confirm the effectiveness of the GA + APC method in minimizing latency across diverse settings. Its exceptional ability to handle real-time mobility, communication constraints, and severe infrastructure challenges makes it an optimal solution for UAV path planning in disaster response scenarios.

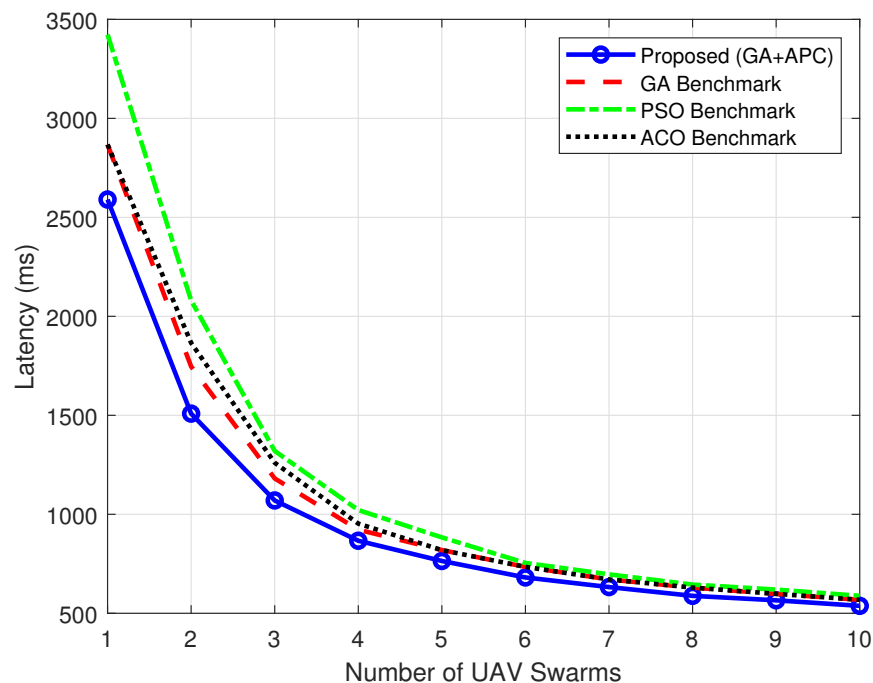


Figure 15. Latency vs. number of UAV swarms in high-rise urban environment.

## 6. Conclusions

This study presents a comprehensive approach for optimizing UAV swarm deployment for DRNs, focusing on enhancing communication coverage, user mobility, and QoS. By combining GA + APC, the proposed method provides a practical and innovative solution to the challenges posed by post-disaster scenarios, where traditional communication infrastructure is often severely compromised.

The evaluation of the proposed approach across various environments, including suburban, urban, dense urban, and high-rise urban scenarios, highlighted its versatility and robustness. Compared with established benchmarks, such as GA, PSO, and ACO, the GA + APC method consistently achieves higher coverage ratios, better QoS compliance, and better fitness scores, even with increasing iterations and diverse mobility models. These results underscore its capability to address the dynamic requirements of real-world DRN applications while ensuring efficient resource utilization.

One of the main findings is the proposed algorithm's adaptability to managing user mobility and challenging environmental conditions. The integration of the RWPM and RPGM mobility models demonstrates their resilience and ability to maintain consistent performance, even as user densities and base station losses increase. This adaptability is critical for ensuring reliable communication coverage during disaster relief operations, where conditions can change rapidly and unpredictably.

Although this study addresses numerous critical challenges, certain aspects remain beyond the scope and represent valuable avenues for future research. For instance, the incorporation of terrain variations and meteorological conditions into the optimization framework will enhance the algorithm's adaptability to real-world scenarios. Subsequent investigations will also explore real-time network demand management utilizing predictive

algorithms to facilitate rapid response to dynamic events. Furthermore, fault tolerance mechanisms such as rerouting strategies and resource redundancy should be developed to ensure uninterrupted connectivity in disaster-affected areas.

Given the significance of UAV energy constraints, subsequent research will incorporate energy-efficient trajectory optimization and renewable energy solutions to extend operational endurance. Furthermore, ensuring user privacy during data collection and relay operations is a critical focus, with plans to implement encryption protocols, privacy-preserving data aggregation, and adherence to privacy standards.

Future research could investigate integrating more advanced machine learning models to enable real-time decision-making and trajectory optimization. Additionally, the potential to incorporate multi-modal communication technologies, such as 5G or satellite integration, could further expand the scope and effectiveness of UAV-enabled networks. Future research could also investigate further optimization of latency in high-rise urban environments and integration with advanced communication technologies, such as 5G, to achieve even better performance.

This study makes a significant contribution to disaster response by introducing a robust and scalable UAV swarm deployment strategy. The proposed GA + APC approach enhances communication reliability and sets a foundation for future advancements in UAV-enabled technologies. Although this study focuses on disaster scenarios, the methodology and insights gained have broader applications, including smart cities, agriculture, and industrial logistics. This study serves as a stepping stone toward more resilient and efficient communication networks, addressing the critical need for innovation in times of crisis.

**Author Contributions:** Conceptualization, N.F.A. and M.S.A.; methodology, M.S.A., N.F.A., and O.A.A.; software, M.S.A.; validation, M.S.A., N.F.A., and A.A.-S.; formal analysis, M.S.A. and N.F.A.; investigation, M.S.A., A.A.-S., and O.A.A.; resources, N.F.A. and R.N.; data curation, M.S.A., A.A.-S., and O.A.A.; writing—original draft preparation, M.S.A. and O.A.A.; writing—review and editing, N.F.A., R.N., and A.A.-S.; visualization, M.S.A. and O.A.A.; supervision, N.F.A. (main supervisor), R.N., and A.A.-S.; project administration, N.F.A. and R.N.; funding acquisition, A.A.-S, N.F.A., and R.N. All authors have read and agreed to the published version of the manuscript.

**Funding:** This work was supported in part by Sunway University’s Research Acceleration Grant Scheme (RAGS; ref: GRTIN-RAG(02)-DEN-03-2024) and the Royal Academy of Engineering, UK (ref: ESMN/2123/2/63 or UKM ref: KK-2022-011).

**Institutional Review Board Statement:** Not applicable.

**Data Availability Statement:** The code used in this research is made openly available in the GitHub repository [https://github.com/Ya-abba/Swarm\\_MABS\\_GA-APC/blob/main/README.md](https://github.com/Ya-abba/Swarm_MABS_GA-APC/blob/main/README.md), accessed on 4 January 2024

**Acknowledgments:** This work would not have been possible without the collective efforts of the team from the Next-Generation Mobile Communication Laboratory, Sunway University and the Wireless Research@UKM from Universiti Kebangsaan Malaysia.

**Conflicts of Interest:** The authors declare no conflicts of interest.

## Abbreviations

The following abbreviations are used in this manuscript:

ACO	Ant colony optimization
AGA	Adaptive genetic algorithms
A	Frequency incidence factor
AR	Angle ratio
$a(hm)$ and Env	Environment correction factors
B	Base station antenna height factor

---

BS	Base station
BPS	Bits per second
bps	Bits per second
Bw	Bandwidth for a channel in Hz
C	Capacity
C	Capacity in bps
CHs	Cluster heads
COW	Cell on wings
CSV	Comma-separated values
D2D	Device-to-device
DCUD	Distributed clustering for user devices
DDQN	Double deep Q-networks
DR	Distance ratio
DRN	Disaster response networks
EH	Energy harvesting
$f$	Frequency in MHz
FPA	Flower pollination algorithm
GA	Genetic algorithm
GHO	Grasshopper optimization
hb	Height of the base station
hm	Height of the mobile aerial base station
HZ	Hertz
ILP	Integer linear programming
IMSIA	Improved multi-objective swarm intelligence algorithm
IoT	Internet of things
IQR	Interquartile range
IR	Intersection ratio
KBPS	Kilobits per second
LOS	Line-of-sight
LTE	Long-term evolution
mMTC	massive machine-type communications
MABS	Mobile aerial base stations
Mbps	Megabits per second
MHZ	Megahertz
MIMO	Multiple-input multiple-output
NLOS	Non-line-of-sight
PL	Path loss
PSO	Particle swarm optimization
PSR	Path smoothness ratio
QoS	Quality of service
RoI	Region of interest
RPGM	Reference point group mobility
RWPM	Random waypoint model
SFOA	Smart flower optimization algorithm
SILC	Swarm intelligence-based localization and clustering
SNR	Signal-to-noise ratio
SINR	Signal-to-interference-plus-noise ratio
SR	Service ratio
UE	User equipment
UAVs	Unmanned aerial vehicles
URLLC	Ultra-reliable, low-latency communication
VD	Voronoi diagram
VDG	Voronoi diagram graph
WPT	Wireless power transfer
$\lambda$	Density value for Poisson distribution

## References

1. Behjati, M.; Zulkifley, M.A.; Alobaidy, H.A.; Nordin, R.; Abdullah, N.F. Reliable aerial mobile communications with RSRP & RSRQ prediction models for the Internet of Drones: A machine learning approach. *Sensors* **2022**, *22*, 5522. [\[CrossRef\]](#) [\[PubMed\]](#)
2. Behjati, M.; Nordin, R.; Zulkifley, M.A.; Abdullah, N.F. 3D global path planning optimization for cellular-connected UAVs under link reliability constraint. *Sensors* **2022**, *22*, 8957. [\[CrossRef\]](#) [\[PubMed\]](#)
3. Qadir, Z.; Ullah, F.; Munawar, H.S.; Al-Turjman, F. Addressing disasters in smart cities through UAVs path planning and 5G communications: A systematic review. *Comput. Commun.* **2021**, *168*, 114–135. [\[CrossRef\]](#)
4. Sánchez-García, J.; Reina, D.G.; Toral, S. A distributed PSO-based exploration algorithm for a UAV network assisting a disaster scenario. *Future Gener. Comput. Syst.* **2019**, *90*, 129–148. [\[CrossRef\]](#)
5. Hydher, H.; Jayakody, D.N.K.; Hemachandra, K.T.; Samarasinghe, T. Intelligent UAV deployment for a disaster-resilient wireless network. *Sensors* **2020**, *20*, 6140. [\[CrossRef\]](#)
6. Liu, H.; Ge, J.; Wang, Y.; Li, J.; Ding, K.; Zhang, Z.; Guo, Z.; Li, W.; Lan, J. Multi-UAV optimal mission assignment and path planning for disaster rescue using adaptive genetic algorithm and improved artificial bee colony method. *Actuators* **2021**, *11*, 4. [\[CrossRef\]](#)
7. Li, J.; Lu, D.; Zhang, G.; Tian, J.; Pang, Y. Post-disaster unmanned aerial vehicle base station deployment method based on artificial bee colony algorithm. *IEEE Access* **2019**, *7*, 168327–168336. [\[CrossRef\]](#)
8. Demir, K.; Tumen, V.; Kosunalp, S.; Iliev, T. A Deep Reinforcement Learning Algorithm for Trajectory Planning of Swarm UAV Fulfilling Wildfire Reconnaissance. *Electronics* **2024**, *13*, 2568. [\[CrossRef\]](#)
9. Montero, E.; Rocha, C.; Oliveira, H.; Cerqueira, E.; Mendes, P.; Santos, A.; Rosário, D. Proactive radio-and QoS-aware UAV as BS deployment to improve cellular operations. *Comput. Netw.* **2021**, *200*, 108486. [\[CrossRef\]](#)
10. Wan, Y.; Zhong, Y.; Ma, A.; Zhang, L. An accurate UAV 3-D path planning method for disaster emergency response based on an improved multiobjective swarm intelligence algorithm. *IEEE Trans. Cybern.* **2022**, *53*, 2658–2671. [\[CrossRef\]](#)
11. Masroor, R.; Naem, M.; Ejaz, W. Efficient deployment of UAVs for disaster management: A multi-criterion optimization approach. *Comput. Commun.* **2021**, *177*, 185–194. [\[CrossRef\]](#)
12. Liu, J.; Liao, X.; Ye, H.; Yue, H.; Wang, Y.; Tan, X.; Wang, D. UAV swarm scheduling method for remote sensing observations during emergency scenarios. *Remote Sens.* **2022**, *14*, 1406. [\[CrossRef\]](#)
13. Zhou, P.; Xie, Z.; Zhou, W.; Tan, Z. A Heuristic Integrated Scheduling Algorithm Based on Improved Dijkstra Algorithm. *Electronics* **2023**, *12*, 4189. [\[CrossRef\]](#)
14. Arafat, M.Y.; Moh, S. Localization and clustering based on swarm intelligence in UAV networks for emergency communications. *IEEE Internet Things J.* **2019**, *6*, 8958–8976. [\[CrossRef\]](#)
15. Hamid, H.; Begh, G. Clustering based strategic 3D deployment and trajectory optimization of UAVs with A-star algorithm for enhanced disaster response. *Phys. Commun.* **2024**, *67*, 102536. [\[CrossRef\]](#)
16. Saif, A.; Dimyati, K.; Noordin, K.A.; Shah, N.S.M.; Alsamhi, S.; Abdullah, Q.; Farah, N. Distributed clustering for user devices under UAV coverage area during disaster recovery. In Proceedings of the 2021 IEEE International Conference in Power Engineering Application (ICPEA), Shah Alam, Malaysia, 8–9 March 2021; pp. 143–148.
17. Javed, S.; Hassan, A.; Ahmad, R.; Ahmed, W.; Alam, M.M.; Rodrigues, J.J. UAV trajectory planning for disaster scenarios. *Veh. Commun.* **2023**, *39*, 100568. [\[CrossRef\]](#)
18. Kamyabniya, A.; Sauré, A.; Salman, F.S.; Bénichou, N.; Patrick, J. Optimization models for disaster response operations: A literature review. *OR Spectr.* **2024**, *46*, 737–783. [\[CrossRef\]](#)
19. Kumar, P.A.; Manoj, N.; Sudheer, N.; Bhat, P.P.; Arya, A.; Sharma, R. UAV Swarm Objectives: A Critical Analysis and Comprehensive Review. *SN Comput. Sci.* **2024**, *5*, 764. [\[CrossRef\]](#)
20. Jain, S.; Bharti, K.K. A combinatorial optimization model for post-disaster emergency resource allocation using meta-heuristics. *Soft Comput.* **2023**, *27*, 13595–13611. [\[CrossRef\]](#)
21. Elnabty, I.A.; Fahmy, Y.; Kafafy, M. A survey on UAV placement optimization for UAV-assisted communication in 5G and beyond networks. *Phys. Commun.* **2022**, *51*, 101564. [\[CrossRef\]](#)
22. Gu, X.; Zhang, G. A survey on UAV-assisted wireless communications: Recent advances and future trends. *Comput. Commun.* **2023**, *208*, 44–78. [\[CrossRef\]](#)
23. Mao, K.; Zhu, Q.; Wang, C.X.; Ye, X.; Gomez-Ponce, J.; Cai, X.; Miao, Y.; Cui, Z.; Wu, Q.; Fan, W. A survey on channel sounding technologies and measurements for UAV-assisted communications. *IEEE Trans. Instrum. Meas.* **2024**, *73*, 8004624. [\[CrossRef\]](#)
24. Pandey, G.K.; Gurjar, D.S.; Yadav, S.; Jiang, Y.; Yuen, C. UAV-Assisted Communications With RF Energy Harvesting: A Comprehensive Survey. *IEEE Commun. Surv. Tutorials* **2024**, early access. [\[CrossRef\]](#)
25. Li, Y.; Zhou, X.; Gu, J.; Guo, K.; Deng, W. A novel K-means clustering method for locating urban hotspots based on hybrid heuristic initialization. *Appl. Sci.* **2022**, *12*, 8047. [\[CrossRef\]](#)
26. Alokaily, M.; Bouachir, O.; Al Ridhawi, I.; Tzes, A. An adaptive UAV positioning model for sustainable smart transportation. *Sustain. Cities Soc.* **2022**, *78*, 103617. [\[CrossRef\]](#)

27. Nafees, M.; Huang, S.; Thompson, J.; Safari, M. Backhaul-Aware UAV-Aided Capacity Enhancement in Mixed FSO-RF Network. *IEEE Open J. Commun. Soc.* **2024**, *5*, 4400–4416. [[CrossRef](#)]
28. Kuru, K. Planning the future of smart cities with swarms of fully autonomous unmanned aerial vehicles using a novel framework. *IEEE Access* **2021**, *9*, 6571–6595. [[CrossRef](#)]
29. Adam, M.S.; Nordin, R.; Abdullah, N.F.; Abu-Samah, A.; Amodu, O.A.; Alsharif, M.H. Optimizing Disaster Response through Efficient Path Planning of Mobile Aerial Base Station with Genetic Algorithm. *Drones* **2024**, *8*, 272. [[CrossRef](#)]
30. Zhong, X.; Huo, Y.; Dong, X.; Liang, Z. QoS-compliant 3-D deployment optimization strategy for UAV base stations. *IEEE Syst. J.* **2020**, *15*, 1795–1803. [[CrossRef](#)]
31. Latifi-Pakdehi, A.; Daneshpour, N. DBHC: A DBSCAN-based hierarchical clustering algorithm. *Data Knowl. Eng.* **2021**, *135*, 101922. [[CrossRef](#)]
32. Alshaibani, W.; Shayea, I.; Caglar, R.; Din, J.; Daradkeh, Y.I. Mobility management of unmanned aerial vehicles in ultra-dense heterogeneous networks. *Sensors* **2022**, *22*, 6013. [[CrossRef](#)] [[PubMed](#)]
33. Pasandideh, F. Providing an Energy-efficient UAV Base Station Positioning Mechanism to Improve Wireless Connectivity. Ph.D. dissertation, Department of Institute of Informatics, Federal University of Rio Grande do Sul, Porto Alegre, Brazil, 2024.
34. Majeed, A.; Hwang, S.O. A multi-objective coverage path planning algorithm for UAVs to cover spatially distributed regions in urban environments. *Aerospace* **2021**, *8*, 343. [[CrossRef](#)]
35. Reina, D.; Camp, T.; Munjal, A.; Toral, S.; Tawfik, H. Evolutionary deployment and hill climbing-based movements of multi-UAV networks in disaster scenarios. In *Applications of Big Data Analytics: Trends, Issues, and Challenges*; Springer: Cham, Switzerland, 2018; pp. 63–95.
36. Madridano, Á.; Al-Kaff, A.; Martín, D.; de la Escalera, A. 3d trajectory planning method for uavs swarm in building emergencies. *Sensors* **2020**, *20*, 642. [[CrossRef](#)]
37. Matamoros Vargas, J.A. Aerial Base Station Deployment for Post-Disaster Public Safety Applications. Master's Thesis, Department of Electrical and Computer Engineering, University of Nebraska-Lincoln, Lincoln, NE, USA, 2019.
38. Beegum, T.R.; Idris, M.Y.I.; Ayub, M.N.B.; Shehadeh, H.A. Optimized routing of UAVs using bio-inspired algorithm in FANET: A systematic review. *IEEE Access* **2023**, *11*, 15588–15622. [[CrossRef](#)]
39. Altay, C.; Koca, M. Design and analysis of energy efficient inter-tier interference coordination in heterogeneous networks. *Wirel. Netw.* **2021**, *27*, 3857–3872. [[CrossRef](#)]
40. Gannapathy, V.R.; Nordin, R.; Abu-Samah, A.; Abdullah, N.F.; Ismail, M. An adaptive TTT handover (ATH) mechanism for dual connectivity (5G mmWave—LTE advanced) during unpredictable wireless channel behavior. *Sensors* **2023**, *23*, 4357. [[CrossRef](#)]
41. Zulkifley, M.A.; Subki, M.G.; Behjati, M.; Nordin, R.; Abdullah, N.F. Mobile Communications and Parachute Systems for Safe Beyond Visual Line of Sight (BVLoS) UAV Operation. In Proceedings of the 2022 IEEE 6th International Symposium on Telecommunication Technologies (ISTT), Johor Bahru, Malaysia, 14–16 November 2022; pp. 22–27.
42. Wang, J.; Gao, Y.; Wang, K.; Sangaiah, A.K.; Lim, S.J. An affinity propagation-based self-adaptive clustering method for wireless sensor networks. *Sensors* **2019**, *19*, 2579. [[CrossRef](#)]
43. Das, S.K.; Roy, S.K.; Weber, G.W. Heuristic approaches for solid transportation-p-facility location problem. *Cent. Eur. J. Oper. Res.* **2020**, *28*, 939–961. [[CrossRef](#)]

**Disclaimer/Publisher's Note:** The statements, opinions and data contained in all publications are solely those of the individual author(s) and contributor(s) and not of MDPI and/or the editor(s). MDPI and/or the editor(s) disclaim responsibility for any injury to people or property resulting from any ideas, methods, instructions or products referred to in the content.